UNCLASSIFIED

SECURITY CLASSIFICATION OF THIS PAGE

DTIC FILE COPY (2)

REPORT DOCUMENTATION PAGE

DTIC ELECTE D 1990

1a

1b. RESTRICTIVE MARKINGS
DISTRIBUTION UNLIMITTED

2a

2b

AD-A219 318

3. DISTRIBUTION/AVAILABILITY OF REPORT
Approved for public release; distribution unlimited.

4.

5. MONITORING ORGANIZATION REPORT NUMBER(S)
AFOSR-TR- 90-0192

6a. NAME OF PERFORMING ORGANIZATION	6b. OFFICE SYMBOL (If applicable)	7a. NAME OF MONITORING ORGANIZATION
Drexel University		AFOSR/NA

6c. ADDRESS (City, State, and ZIP Code)	7b. ADDRESS (City, State, and ZIP Code)
32nd and Chestnut Street Philadelphia, PA 19104	Building 410 Bolling AFB, DC 20332-6448

8a. NAME OF FUNDING/SPONSORING ORGANIZATION	8b. OFFICE SYMBOL (If applicable)	9. PROCUREMENT INSTRUMENT IDENTIFICATION NUMBER
AFOSR/NA	NA	AFOSR-88-0113

8c. ADDRESS (City, State, and ZIP Code)	10. SOURCE OF FUNDING NUMBERS			
	PROGRAM ELEMENT NO.	PROJECT NO.	TASK NO.	WORK UNIT ACCESSION NO.
Building 410 Bolling AFB, DC 20332-6448	61102F	2302 (A)	B2	

11. TITLE (Include Security Classification)
A COMPREHENSIVE STUDY ON MICROSTRUCTURE_MECHANICS RELATIONSHIPS OF CERAMIC MATRIX COMPOSITES

12. PERSONAL AUTHOR(S)
A.S.D. Wang and M. W. Barsoum

13a. TYPE OF REPORT	13b. TIME COVERED	14. DATE OF REPORT (Year, Month, Day)	15. PAGE COUNT
Final Technical Repor	FROM 1 Apr 88 TO 30 Jun 89	20 Dec 1989	63

16. SUPPLEMENTARY NOTATION

17. COSATI CODES			18. SUBJECT TERMS (Continue on reverse if necessary and identify by block number)
FIELD	GROUP	SUB-GROUP	
			Ceramic matrix composites; Matrix cracking ~~initiation~~; Specimen fabrication; Testing; Theory; Simulations, unaxial fiber, Fracture Mechanics, C.O. [illegible]

19. ABSTRACT (Continue on reverse if necessary and identify by block number)

The background of this research stems from the need to understand the physical mechanisms of brittle matrix cracks in fiber reinforced ceramic matrix composites. Three major tasks are performed during the research: (1) an in-house fabrication facility is established; (2) a testing technique is developed; and (3) a theory for matrix crack initiation and a numerical simulation method is formulated. A preliminary correlation between theory and experiment is accomplished.

This report contains two individual technical papers; one describes the details of the experimental aspects and the other describes the theoretical and the simulative aspects.

20. DISTRIBUTION/AVAILABILITY OF ABSTRACT	21. ABSTRACT SECURITY CLASSIFICATION
☑ UNCLASSIFIED/UNLIMITED ☑ SAME AS RPT. ☐ DTIC USERS	UNCLASSIFIED

22a. NAME OF RESPONSIBLE INDIVIDUAL	22b. TELEPHONE (Include Area Code)	22c. OFFICE SYMBOL
[redacted] George K. Haritos	[redacted]	NA

DD FORM 1473, 84 MAR 83 APR edition may be used until exhausted
All other editions are obsolete

SECURITY CLASSIFICATION OF THIS PAGE

☆U.S. Government Printing Office: 1985-607-047

(300767 0463)

UNCLASSIFIED

18 JAN 1990

A COMPREHENSIVE STUDY ON MICROSTRUCTURE-MECHANICS RELATIONSHIPS OF CERAMIC MATRIX COMPOSITES

A.S.D. Wang and Michel Barsoum
Drexel University
Philadelphia, PA 19104

FINAL TECHNICAL REPORT

GRANT NO. AFOSR-88-0113

for

Director of Aerospace Sciences
Air Force Office of Scientific Research
Bolling AFB, DC 20332

December 1989

90 02 23 058

INTRODUCTION

This report contains the results of the research supported by Air Force Office of Scientific Research under the Grant AFOSR-88-0113 to Drexel University. The Grant covers the period from 1 April 1988 to 30 June 1989.

The background of this research stems from the need to understand the physical mechanisms of brittle matrix cracks in fiber reinforced ceramic matrix composites, which are being developed in recent years as a structural material for high temperature applications. Since matrix cracks in such composites often form at very low strains, due to the brittle nature of ceramic matrix, it falls short of the expectation that such composites can be safely used as a high-strength and high-temperature structural material. On the other hand, ceramics have been proven to function structurally in high temperature environments if they can be made relatively free of flaws. In the case of ceramic matrix reinforced with high strength fibers, the potential of the fibers is expected to be fully realized. This, however, depends largely on whether or not an optimum fiber-matrix interfacial bond is provided. It has been known that the effectiveness of interfacial bond may be adversely affected by the existence of flaws both in the matrix and in the interface. The degree to which matrix cracking depends on the effectiveness of interfacial bond is a subject of current research.

The present study is aimed at the mechanics relationship linking interfacial bond, flaws and other microstructural factors in the formation of matrix cracking.

OBJECTIVES OF RESEARCH

The main objectives of the research are: (1) to establish an in-house capability by which a class of high temperature ceramic matrix composite materials can be fabricated with the ability to control some of the most important microstructural factors; (2) to establish a mechanical testing procedure by which composite specimens are tested and examined for matrix cracking against the background of varied factors; and (3) to develop a physical damage theory, accounting for all the influential factors, whereby a mathematical (numerical) method can be formulated

COPY INSPECTED
For
ty Codes
Avail and/or
Dist Special
A-1

which simulates matrix cracking in the tested specimens.

These objectives serve as the basis of the current research, which involves close collaboration and interaction between the material science discipline and the mechanics of solids discipline.

ACCOMPLISHMENTS

Fabrication. During the course of the present research, a 50-ton/ 1500°C hot press was setup for the fabrication of SiC fiber reinforced glass matrix composites. The fabrication technique is similar to that developed by Haller, et. al. [1]. Briefly, the Haller procedure involves coating the fiber filament with a slurry containing a UV (ultraviolet) curable polymer, mixed with the glass powder. The coating is achieved by drawing the fiber through the prepared slurry (contained in a bath) and exposing it immediately to UV light for curing. The coated fiber is then cut into desired length; and the cut fibers are laid out with the prescribed fiber packing pattern inside a die. The polymer is carefully burnt out and the system is vacuum pressed (in the hot press) at the prescribed temperature. For the various glass materials (borosilicates) used in this research, it was found that the ideal hot pressing temperature is the working temperature of the glass matrix (set around 1200°C). Lower hot pressing temperature can result in insufficient flow of the glasses, while higher temperature causes crystallization of the glasses.

By the above procedure, unidirectional composite specimens were fabricated successfully using three fiber-matrix combinations, with control and variation of several microstructural variables, such as fiber diameter, interfiber spacing, etc. These factors are found to play an important role in the initiation and progression of matrix cracking in the composites.

Matrix Cracking Test. A testing technique was developed for inducing matrix cracking in the test specimen and for determining the critical load at matrix cracking. The mechanical test involves specimens in the form of a beam (approximate lenth-width-thickness dimensions: 3x0.5.x0.2 cm) which is loaded in 3-point or 4-point bending by an Instron tester. In order to measure the matrix cracking event during loading, the tensile surface of the beam-specimen is first polished down to

0.05 mm using alumina powder (Linde B) to remove any glassy surface residue due to fabrication. A 1000 nm thick gold film is then sputtered on the polished surface. The electrical resistance of the gold film is measured during the test in real-time; and a sudden increase in the resistance identifies the initiation of matrix cracking. The novel testing and recording technique has several advantages. First, the 3-point bend test is relatively easier to conduct than the simple tension test, especially when the testing is carried in severe temperatures. Secondly, the gold film technique provides an excellent sensitivity in detecting the onset of matrix cracking in real time and the technique can be applied reasonably well in severe testing temperatures.

In the present research, specimens from three fiber-matrix combinations were tested for matrix crack initiation. These three combinations are (1) Nicalon SiC/LAS system with 50 v% fiber; (2) AVCO SiC/ borosilicate glass system with 17 v% fiber; (3) Hercules HMU graphite/borosilicate system with 45 v% fiber and 50 v% fiber. These four types of specimens provided a reasonable spread of variation in some of the important microstructural factors. And, indeed, the corresponding critical matrix cracking stresses also varied appreciably.

A detail account of the experimental work has been presented in conferences and/or seminars, and published in a paper [2] which is appended to this report. The paper was recently submitted to the Journal of Material Science for publication.

Matrix Cracking Theory and Simulation. For matrix cracking in unidirectionally fiber reinforced composites, a micromechanics analysis based on the concept of brittle fracture was first introduced by Aveston, Cooper and Kelly in 1971 [3]. Their analysis, widely known as the ACK model, assumes that a fiber-bridged matrix crack of sufficient size already exists in the composite, and that it will propagate steadily as a fiber-bridged crack under a certain uniformly applied stress condition. That condition, which determines the critical matrix cracking stress, is governed by an energy balance during the course of the propagation. In writing the energy balance equation, ACK considered the strain energy released by the cracking matrix, the work done in debonding the fiber-matrix interface as well as the frictional work due to fiber sliding against the matrix. Thus, several factors at the fiber-matrix level could be

included in the energy equation.

The ACK model, however, has not been thoroughly validated by experiment despite of it's nearly 20 years of existence. One possible reason is that the phenomenon of fiber-bridged matrix crack does not generally occur in polymer matrix composites, which are the main structural composites in use in the past 20 years.

The study of fiber-bridged matrix cracking in ceramic composites attracted research attention only in recent years. And, there have already been several refinements [4,5] of the ACK model. There is clearly a need to experimentally validate the ACK model as well as it's derivative models. With the matrix cracking tests performed in this research, a preliminary check of the ACK model thus became possible.

The main contribution in the present research is the proposition of a different view point on how a matrix crack is initiated. The basis of the proposition is the assumption that the composite is fabricated along with randomly distributed flaws, both in the matrix material and in the fiber-matrix interface; the matrix flaws act like small starter cracks which propagate and coalesce to form the observed fiber-bridged matrix cracking. The presence of the interfacial flaws is deemed to dominate the fundamental character of the matrix cracking mechanisms.

By applying the basic concept of brittle fracture and in conjunction with a probabilistic distribution of flaws, a numerical simulation model has been developed based on the above matrix cracking proposition and applied to the tests conducted in this research. Thus, a preliminary validation of the new model became also possible.

Results of this part of the research have been presented in several technical conferences during the past year; a comprehensive paper [6] describing the development background of the various matrix cracking theories and the details of the present simulation model is appended to this report. The paper has recently been submitted to the Journal of Composite Materials for publication.

FUTURE WORK

The research results reported herein represent the first phase of a large effort

to understand the physical mechanisms of matrix cracking in fiber reinforced ceramic matrix composites. Much more experiment and simulations remain to be performed in order to adequately determine the relative influence of those factors already identified and those factors yet to be discovered. Ultimately, one must also venture into the realm of high temperature, which is a major reason behind the development of ceramic matrix composites.

REFERENCE

[1] Haller, W., Deshmukh, U. and Freiman, S.,"Novel Process for Preparation of Fiber Reinforced Ceramic Matrix Composites," J. Amer. Ceramic Society, Vol. 71, 1988. C-498-500.

[2] Barsoum, M. and Plotnick, B., "Matrix Cracking Stresses in Uniaxially Fiber Reinforced Ceramic Composites," submitted to Jour. Materials Science. (appended in this report).

[3] Aveston, J., Cooper, G. and Kelly, A, "Single and Multiple Fracture," in The Properties of Fiber Composites, Conference Proceedings, National Physical Laboratory, Guildford, UK. IPC Science and Technology Press Ltd., 1971, pp. 15-26.

[4] Marshall, D., Cox, B. and Evans, A.,"The Mechanics of Matrix Cracking in Brittle-Matrix Fiber Composites," Acta Metall., Vol. 33, 1985, pp. 2013-2021.

[5] McCartney, L. N., "Mechanics of Matrix Cracking in Brittle-Matrix Fiber-reinforced Composites," Proc. Roy. Soc. London, A-409, 1987, pp. 329-350.

[6] Wang, A. S. D., Barsoum, M. W. and Huang, X. G., "Matrix Cracking Initiation in Brittle Matrix Composites," submitted to Jour. Composite Materials. (appended in this report).

APPENDIX

1. "Matrix Cracking Stresses in Uniaxially Fiber Reinforced Ceramic Composites."
   Paper presented by M. Barsoum at
   The 91th ACS Annual Meeting, May 1-5, 1989, Indianapolis, IN. (71-SI-89)
   Tokyo Institute of Technology, September 1988, Tokyo, Japan
   Rutgers University, Piscataway, NJ, October 1989.
   Paper submitted to Jour. Materials Science, June 1989.

2. "Matrix Cracking Initiation in Brittle Matrix Composites,"
   Paper presented by Wang at
   The 1st USSR-USA Symposium on Mechanics of Composite Materials, May 25-29, 1989, Riga, Latvian SSR.
   Symposium on High Temperature Composites, American Society for Composites, June, 1989, Dayton, OH.
   Virginia Polytechnic Institute and State University, October 1989.
   Paper submitted to Jour. Composite Materials, October 1989.

Preprint: Please do not cite or reference

Matrix Cracking Stresses in Uniaxially Fiber Reinforced Ceramic Composites

by
Michel Barsoum‡ and Bruce Plotnick
Department of Materials Engineering
Drexel University
Philadelphia, Pa. 19104

ABSTRACT

The stress at which the first matrix cracks occurs in fiber reinforced ceramic composites was determined by measuring the electrical resistance changes of a thin gold film sputtered on the surface of the composite as a function of applied stress in three point bend tests The matrix cracking stress (MCS) for a SiC-LAS composites (50 v%) was found to be 370±10 MPa. In some cases, cracks due to fibers breaking were observed prior to the onset of the matrix cracks, the presence of which did not influence the MCS, however. In contrast to the matrix cracks that closed easily upon removal of the stress, the cracks associated with the broken fibers and the cracks parallel to the fibers did not. Heating in air resulted in the formation of a glass-like layer on the surface of the composite. Mild etching in dilute HF had little effect on the MCS of the LAS matrix composite. The MCS of a 43 vol% C-fiber reinforced borosilicate matrix composite was measured to be 360±2 MPa. Mild etching (120s in 5%HF) resulted in an almost twofold increase in the MCS to over 650 MPa, most probably due to chemical etching of the surface and the concomittant reduction in the size of the prexisting surface flaws. For a borosilicate matrix-17 v% SiC fibers the matrix cracking stress was found to be 78±10 MPa. In addition to the matrix cracks localized cracks due to fiber breaks andcracks parallel to the fibers were detected.

‡ Member Amer. Cer. Soc.

Key Words: Matrix cracking stress, uniaxial fiber reinforced ceramic composites, fracture mechanics, oxidation, fiber breaks, HF etching.

INTRODUCTION

It has long been appreciated that the reinforcement of brittle matrices with high strength fibers can result in dramatically improved properties such as increased toughness and large tensile strains to failure. Recently the development of silicon carbide type fibers and others such as alumina, has led to a major resurgence of interest in fiber reinforced ceramic matrix composites for high temperature applications. Fiber reinforced ceramics offer advantages of high strength and stiffness coupled with low density, moderate toughness and hardness. With proper tailoring of the interfacial shear stress, the addition of fiber reinforcement offers significant potential advantages over monolithic and whisker reinforced ceramics in that they will not fail catastrophically.

Though the ultimate load bearing capacity of uniaxially reinforced composites usually exceeds the load for the formation of the first matrix cracks, it is the latter which is of prime importance because it signifies the onset of permanent damage and the loss of protection provided by the matrix against oxidation or corrosion of the fibers. Hence, the matrix cracking stress, MCS, is the likely design stress. Furthermore, the MCS plays an extremely important role in the overall mechanical performance of these composites. For example, Prewo(1) has shown that cycling at stresses higher than the MCS at elevated temperatures (600-1000 °C) resulted in a noticeably embrittled composite fracture mode as a result of the atmosphere penetrating the composite. Even at room temperature a change in composite stress-strain behavior was induced.

Whereas no standard technique to determine the MCS exists, several investigators(2-6) have related the stress at which the stress-strain curves, in either uniaxial tension or flexure, become nonlinear to the matrix cracking stress. Table I summarizes the matrix cracking stresses recently reported for C and SiC fiber reinforced glasses and glass ceramics from which it is apparent that a wide variability in the measured values of MCS exists. One of the motivations of this work has been to try and understand some of the underlying mechanisms and important microstructural features

responsible for the initiation of matrix cracks.

The disadvantages of the tensile test are several and include fabricating relatively large samples with the concomitant need for a large amount of material, machining requirements and gripping problems. A further complication is the fact that as the volume fraction of the fiber decreases, the point at which the discontinuity in the stress-strain curves occurs becomes less well defined(5). This problem is even more severe during flexure: more often than not, the exact stress at which the curves become nonlinear is not easy to determine. Kim and Pagano(7) also showed that the association of the point of initial nonlinearity of a stress strain curve with the MCS is incorrect in a number of composites. Furthermore, both tests only yield information on a macroscopic scale and do not yield information about other failure modes that could be occurring before or during matrix cracking such as fibers breaks or delamination cracks, damage evolution, anisotropy of cracks formed, etc.

In this paper the matrix cracking stresses of three fiber reinforced ceramic composites were measured by monitoring the electrical resistance changes of a thin gold film sputtered on the surface of the composite as a function of applied stress in three and four-point bend tests. In addition to incorporating all the advantages of the flexure testing, i.e. simplicity of test, small volume requirements, etc., the onset of matrix cracking can be unambiguously and accurately measured, even at low volume fraction fibers, as well as information concerning other types of cracks formed and their anisotropy.

THEORY

Matrix Cracking Stress

Aveston, Cooper and Kelly(9) developed a theory which explains the suppression of cracking in fiber composites by considering the energy requirements for the production of matrix cracking. In this model the failure strain in a low failure strain matrix is given as:

$$\varepsilon_m = \left[\frac{12\,\gamma_m \tau\, E_f\, V_f^2}{E_c\, E_m^2\, V_m\, R} \right]^{1/3} \qquad \text{----------} (1)$$

where $E_c = V_f E_f + V_m E_m$, τ is the shear strength of the interface, E_f, V_f, E_m, V_m are, respectively, the Young's moduli and volume fractions of matrix and fiber. R is the radius of the fibers and γ_m is the fracture surface energy of the matrix.

Using a fracture mechanics analysis Marshall, Cox and Evans (10) derived the following equation for the stress at which matrix cracking will occur:

$$\sigma_o = \left[\frac{6\,(K_c^m)^2\, \tau\, E_f\, V_f^2\, V_m\, \eta^2}{E_m\, R} \right]^{1/3} \qquad \text{----------(2)}$$

where η is given by:

$$\eta = 1 + \frac{E_f V_f}{E_m V_m}$$

and K_c^m is the fracture toughness of the matrix defined as $\sqrt{2}\,\gamma_m E_m$. Eqs. 1 and 2 are related since:

$$\sigma_o = \varepsilon_m E_c$$

Values of σ_0 calculated for the three composite systems used in this work are listed in Table 2.

It is important to note that Eqs. 1 and 2 are only valid for the extension of large cracks. Eq. 2 is only applicable when the crack length is of the order of $c_m/3$ where c_m is a characteristic crack length given by(9):

$$c_m = \left(\frac{\pi}{4 I^{4/3}} \right) \left[\frac{K_c^m\, E_m\, V_m^2\, \eta\, R\, (1-\nu^2)}{\tau\, V_f^2\, E_f} \right]^{2/3} \qquad \text{----------(3)}$$

where I is a dimensionless crack geometry constant = 1.2 for straight cracks and 0.66 for

penny cracks.

Furthermore, the stress, σ, required to propagate cracks with $c < c_m$ will be greater than the steady state value, σ_o, given in Eq.2, according to(10):

$$\frac{\sigma}{\sigma_m} = \frac{1}{3}\left[\frac{c}{c_m}\right]^{-1/2} + \frac{2}{3}\left[\frac{c}{c_m}\right]^{1/4} \qquad \text{----------(4)}$$

where $\sigma_m = 0.98\,\sigma_o$ for straight cracks and $\sigma_m = \sigma_o$ for penny shaped cracks. Thus for cracks shorter than $\approx c_m/3$ the stress required to cause matrix fracture increases as the crack length decreases with a crack length dependence resembling that of a monolithic brittle material.

Recently, McCartney(11), considering only straight cracks and using a slightly different fracture criteria than Marshall et. al.(10), obtained a result for long cracks that is identical to Eq. 2. Where the anaylsis of McCartney differs from Marshall's et al. is in the estimation of c_m. The characteristic flaw size, a_o, in McCartney's analysis is given by:

$$\sigma_f \sqrt{(\pi a_o)} = K_{1c}$$

where K_{1c} is defined as:

$$K_{1c} = \left[\frac{V_m E_c}{E_m}\right]^{1/2} K_{1c}^m$$

σ_f is 0.75 the value calculated from Eq. 2. It should be pointed out that c_m and a_o are not directly comparable. In McCartney's model, the validity of Eq. 2, is only established when $a/R \approx 10$, where a is the size of the prexisting crack size.

Experimental Procedure:

Three unidirectional fiber reinforced composite systems, the properties of which are listed in Table II, were tested:

i) SiC/LAS (50 v% SiC Nicalon fiber, manufactured by UTRC).

ii) C/borosilicate (43 v% C - Hercules HMU fiber, manufactured by UTRC).

iii) SiC/borosilicate (17 v% SiC, AVCO fibers). This composite was made by suspending the borosilicate glass powder (Corning 7740) in a slurry containing an ultraviolet light curable polymer. The fibers were then individually coated with the slurry, subjected to ultraviolet light, sectioned to appropriate size and stacked to obtain the desired composite thickness. The binder was burned out and the composite was hot pressed. More details on the fabrication process are published elsewhere (12).

The composite samples were cut into smaller bars suitable for three point bending. The size of the samples varied but were roughly 3 x 0.5 x 0.18 cm for the LAS/SiC, 3 x0.5 x 0.44cm for the SiC/borosilicate and 3x 0.5 x 0.2cm for the C/borosilicate samples. The span of the lower support pins was 2.54 cm, yielding a span-to-depth ratio varying from 6-14. The tensile surface of the bars were sputtered with a 1000 nm thick gold film that covered the width of the samples and onto which line contacts normal to the applied stress were attached using a conductive epoxy paste as shown schematically in Fig.1a. In one sample, point contacts were placed in a cross pattern (Fig.1b) normal and parallel to the applied stress in an attempt to measure the anisotropy of crack formation. The electrodes for all the other samples were line electrodes as shown in Fig. 1a. The load was applied using a manually operated soil tester (U-160 Soiltest, Inc., Chicago Ill.) and converted to a stress assuming a uniform elastic beam in bending.

It was necessary to polish the samples prior to testing in order to remove the thin glass layer that was present on the surface and to expose the underlying matrix/fiber surface. If not removed, the fracture of this glass layer dominated the response of the gold film and masked the response of the composite (see Appendix A). All samples were thus polished down to 0.05 μm alumina powder (Linde B) prior to the sputtering of the gold film. The experimental technique used in this work, and detailec elsewhere(8), is

based on measuring the electrical resistance changes of a sputtered gold film as a function of applied stress. In our previous work, the onset of matrix cracking was clearly manifested by a sudden and dramatic increase in the normalized resistance changes, $\Delta R/R_o$, as a function of the maximum applied stress, σ_{max}, in three point bend tests. Due to the fact that, in some cases, polishing resulted in fiber damage which tended to mask the onset of matrix cracking, a slightly modified loading procedure, discussed in more detail in the Appendix, was used. In summary, the load was cycled as shown in Fig. 1c, and the resistance at maximum load, R_{max} , and minimum load, R_{res}, were measured. Since the cracks associated with the fiber breaks do not close upon removal of the load whereas the matrix cracks do, plotting the difference $(R_{max} - R_{res})/ R_o$, where R_o is the initial resistance of the gold film, was found to better delineate the point at which matrix cracking occurred.

In an attempt to examine the effect of surface finish on the MCS, some of the samples were etched in 5% HF for various times, rinsed in water and air dried prior to sputtering the gold.

One of the LAS samples was oxidized in air at 1000 °C for 24 hours prior to gold coating.

A small three-point bend assembly that would fit in an SEM was fabricated and used for post-test examination of the gold plated surfaces. The samples were placed in the sample holder and examined in the SEM, with and without load and the various failure modes were identified.

RESULTS

SiC/LAS

Typical results for the LAS/SiC composites are shown in Fig. 2 where both $\Delta R_{max}/R_o$ and $\Delta R_{res}/R_o$ ($\Delta R_{max} = R_{max}-R_o$ and $\Delta R_{res} = R_{res}-R_o$) are plotted versus

σ_{max}. Two samples were tested; in 3 and 4-point bending (the 4-point data is shifted by 0.1 vertically for the sake of clarity). In both cases, two regimes are obvious: initially the resistance increases very slowly but linearly with stress, but in both cases, at ≈370 MPa , $\Delta R_{max}/R_o$ increases dramatically with stress. As discussed in more detail later, this increase corresponds to the MCS.

The results for the sample tested with the 4-point electrodes (Fig. 1b) are shown in Figs.3a and b for both the parallel and normal directions to the applied load, respectively. This sample was not mounted during polishing and consequently, similar to all unmounted samples (see Appendix), exhibited three regions instead of two. In region I, the resistance changes are very small and increase linearly with applied stress. Region II is characterized by a simultaneous increase in both $\Delta R_{max}/R_o$ and $\Delta R_{res}/R_o$; i.e. the resistance changes do not recover upon unloading . Region III is characterized by a large divergence between $\Delta R_{max}/R_o$ and $\Delta R_{res}/R_o$. Note the absence of a sharp break in the $\Delta R_{max}/R_o$ vs σ_{max} curve. However, when the data was replotted as $(R_{max} - R_{res})/ R_o$ a much sharper break results (see Fig. 4)

Comparing Figs. 3a and b, it is clear that whereas the absolute values of $\Delta R_{max}/R_o$ are greater in the normal direction, the divergence between $\Delta R_{max}/R_o$ and $\Delta R_{res}/R_o$ is greater in the parallel direction.

A total of 8 LAS/SiC samples were tested and the results are summarized in Fig. 4 where, with the exception of one sample, a sharp increase in $(R_{max}-R_{res})/R_o$ at 370± 10 MPa was observed

b) Borosilicate/SiC

The stress dependance of $(R_{max}-R_{res})/R_o$ for the three SiC borosilicate samples tested are also plotted in Fig. 4. The increase in resistance was observed at 78±10 MPa.

c) Borosilicate/C-fiber

$\Delta R_{max}/R_o$ versus σ_{max} curves for the borosilicate/C-fiber system are summarized in Fig. 5a as a function of etching time. The point at which $\Delta R_{max}/R_o$ increases dramatically increases from 360 MPa, for the as-received and polished samples, to over 650 MPa after 120 s etch. The sample etched for 120 s did not fail by the formation of matrix cracks normal to the applied stress, but rather in what appears to be have been a torsional failure: post test examination revealed a large crack parallel to the fibers.

The effect of etching on the onset of matrix cracking were much less pronounced for the LAS composite system as shown in Fig. 5b. The MCS drops from 360 MPa before etching to 310 MPa after a 30 s etch and then slowly rises with increasing etching time.

Effect of Oxidation

In order to examine the effect of oxidation on the properties of the LAS composite one sample was polished and placed in a furnace at 1000°C for 24 hrs and furnace cooled. Microstructural observation of the surface after oxidation, but prior to testing, showed that the originally polished surface in which the fibers were clearly visible could no longer be distinguished from the unpolished surface and seemed to have been covered by a thin glassy layer. The stress dependence of the resistance after oxidation was similar to the response of the as-received samples prior to polishing (see Flg. A1 in Appendix). After the same sample was repolished and a new gold film deposited, the resistance changes were markedly different and resembled the results shown in Fig. 3.

MICROSTRUCTURAL OBSERVATION

A typical tensile surface, under stress in the SEM, of a LAS/SiC sample loaded past region II is shown in Figs.6 a & b. In Fig. 6a a series of roughly equally spaced matrix cracks running through the matrix normal to the fibers are visible; the spacing between the cracks is about 450 μm. At higher magnifications (Fig. 6b), in addition to the matrix cracks, a number of cracks associated with broken fibers are also visible. When the same sample was observed without load, the matrix cracks could only be seen at very high magnifications (15000 x) and were very difficult to locate, whereas the cracks associated with the broken fibers were still easily discernible.The matrix cracks were only observed when a divergence between $\Delta R_{max}/R_o$ and $\Delta R_{res}/R_o$ occurred. When the experiments were interrupted in region II, only broken fibers, which were readily seen even without loading, were observed as shown in Fig. 7a. The matrix cracks for the C/borosilicate composite sample that was etched for 60 s are shown in Fig.7b and are quite similar to those shown in Fig. 6, except that it appears that more fibers are broken.

When the sample onto which the 4 electrodes were placed was observed, under load, in the SEM cracks running parallel to the fibers were observed (Fig. 8a). When the load was removed these cracks were still easily observable. A similar type of crack was found for the borosilicate sample that was etched for 120 s: a large crack, shown in Fig. 8b, was observed.

DISCUSSION

Matrix Cracking Stress

The correlation between the presence of matrix cracks with the point at which $(R_{max} - R_{res})/R_o$ starts increasing offers compelling evidence that this technique can be used to accurately and reproducibly measure the onset of matrix cracking in uniaxial ceramic composites using flexure tests. In addition to the advantages inherent in using three point-bend tests, SEM post-test examination of the damaged surface is readily carried out, in contrast to strain gauges that tend to mask the surface. Furthermore, with a slight modification of the loading cycle and/or placement of the electrodes, it is possible to differentiate between various types of crack, such as individual fibers breaking or cracks parallel to the fibers.

The SEM observations confirmed that the matrix cracks close easily as the stress is removed, which explains why the resistance changes associated with the matrix cracks are recovered upon unloading. These cracks close readily because they are linked to the undamaged matrix below the surface of the composite which pulls them together upon unloading. No such traction forces are operative when single fibers break and explains why the resistance changes associated with them are not recovered upon removal of the stress. The need to load the specimens to observe the matrix cracks was made by others as well; for example Marshall and Evans [3] using in situ observations during flexure observed that upon removal of the load the matrix cracks were no longer visible. Mah et al. [2] also failed to observe matrix cracks without loading the sample.

A total of 8 samples were tested for the LAS/SiC composite, 2 tests were interrupted before region III, 5 exhibited a MCS of 370 ±10 MPa, and 1 at about 290 MPa. The value of 370±10 MPa reported here is well within the values quoted for the MCS in the literature for the same system and similar volume fractions (see Table I). The reason for the large variations in MCS shown in Table 1 for similar samples is not well understood but could reflect either variations in τ due to variations in the processing parameters, or the effect of residual stresses, or they could reflect variations in the size and nature of the preexisting surface cracks. The latter is most likely however, since improper composite processing can result in the presence of matrix defects either due to insufficient flow of the matrix around the fibers during consolidation or cracks that are generated due to thermal stresses upon cooling. The presence of a large surface crack could explain the lower MCS measured for the sample that failed at 290 MPa in Fig. 4.

By comparing the results shown in Fig. 2 and 3, it is clear that the MCS was not a function of the extent of surface fiber damage, as measured by the value of $\Delta R/R_o$ just before matrix cracking, implying that the stress intensity factors associated with broken fibers are not as severe as the ones associated with prexisting matrix cracks.

For the 17 v% AVCO/borosilicate matrix composite 3 samples were tested and the MCS was found to occur at 78 ±10 MPa (Fig. 4). It is worth noting that using this technique, the difficulty of accurately determining the point at which load-deflection curves become nonlinear and hence the MCS, especially at low fiber volume fractions is eliminated(5).

The MCS for the C/borosilicate composites was 360±2 MPa. This value agrees well with the values reported by Prewo(5) for the same composite system using tensile specimens (see Table 1), and indicates that the matrix cracking stress is insensitive to the type of loading. This is also confirmed by the results shown in Fig. 2 where the same MCS was obtained in 3 and 4-point tests. However, it should be pointed out that this conclusion is not valid past the stress at which the matrix cracks since flexural specimens have been known to fail by buckling on the compressive side(3).

When the experimental results are compared with the theorectical predictions the agreement is rather poor (Table 2) . While it is possible to rationalize values of MCS that are higher than the theoretical values by assuming flaw sizes that are smaller than $c_m/3$, the theory does not allow for MCS values that are lower than the value given by Eq. 2 which is the steady state or large crack size configuration. The differences between the experimental and theoretical values for the C system are quite significant. While there is some uncertainty as to the value of τ in this system that ranges from 10 MPa (3) to 25 MPa (5), assuming the lower value, σ_0 is calculated to be 584 MPa which is significantly higher than the measured value of 360 MPa.

The Effect of Etching

It is well known that etching of glass will increase its strength by eliminating, blunting or reducing surface flaws. A similar effect is the most probale reason for the almost twofold increase in MCS as a result of etching of the C/borosilicate matrix (Fig. 5a). The results also imply that, at least in three point bending, the matrix cracks are surface initiated. From a practical point of view this result is not very significant since service induced flaws would tend to reduce the MCS. However, the results suggest that if it were possible to manufacture composites with surfaces finishes approaching those achieved by etching and subsequently protect these surfaces, very high strength could be achieved.

Why etching of the LAS composite resulted in a much less pronounced effect on the MCS (Fig. 5b) than for the C/borosilicate matrix composites is not entirely clear. One possibility is that the fracture origin in the LAS composite are the grain boundries which cannot be etched away. The initial drop in MCS, from 360 MPa (unetched) to 310 MPa after 15 s could be due to the etching away of the glass phase at the grain boundary creating flaws. Etching for longer times could tehn possibly blunt these cracks which would explain the slight increase in MCS obreved at longer etching times.

Anisotropy of Cracks Formed

The divergence between $\Delta R_{max}/R_o$ and $\Delta R_{res}/R_o$ in both normal and parallel to the applied stress direction was found to occur at the same stress, namely 360 MPa (Fig.3a and b), which idicates that simultaneous with the formation of the matrix cracks, cracks running parrallel to the fibers are also formed. The fact that the absolute value of $\Delta R_{max}/R_o$ parallel to the applied stress direction is greater than in the normal direction is consistent with theSEM observation that the matrix cracks are bridged by fibers whereas the cracks parallel to the fibers are not; the bridging fibers provide a path for the current hence reducing the absolute value of $\Delta R_{max}/R_o$ in that direction. The parallel cracks could result from a Poisson contraction of the fibers upon matrix cracking: as the load is transferred to the fibers, the resultant Poisson contraction would place the fiber/matrix interface in tension and thus cause delamination. Judging from the SEM micrographs the delamination failure mode is as severe and potentially as damaging if not more damaging than the matrix cracks since they occur along a weak interface. Such cracks would also be more susceptible to fatigue and thermal cycling.

Since the traction forces are smaller in the parallel than in the normal direction the parallel cracks do not close as easily as the matrix cracks as evidenced by the much smaller divergence between $\Delta R_{max}/R_o$ and $\Delta R_{res}/R_o$. In general, the resistance changes are a function of the film geometry (8) however, the results shown in Fig. 3, are directly comparable because in this case a square film geometry was used. It should be pointed out that the parallel cracks were not observed for all samples in the SEM, and it is possible that these cracks resulted from the constraints placed on the matrix due to the electrodes used to measure them (see Fig. 1b). Since only one test was performed with the 4-electrode configuration, it is not possible to draw any general conclusions concerning the simultaneous formation of parallel and matrix cracks, however, given the fact that τ is quite low in the SiC/LAS system such cracks are to be expected. Furthermore, it has previously been shown that in cross-plys of the same system both types of cracks are present and occur simultaneously(8).

Effect of Oxidation

As mentioned earlier, prior to oxidation, the tensile surface of the samples was carefully polished so that the fibers and matrices were clearly distinguishable. After oxidation, however, the polished surface was no longer distinguishable from the non-polished or the as-received surfaces and a thin glass layer seemed to have formed on the surface. Upon loading this brittle oxidation layer cracked easily and resulted in the immediate increase in resistance observed (see Fig. A1 in Appendix). Repolishing removed part of the brittle layer and consequently the shape of the curves after repolishing

resemble more closely those of the unoxidized samples, and the break in the curve at ≈360 MPa was recovered.

This conclusion is in accord with previous investigations (1,14,15) that have shown that oxidation resulted in severe embrittlement of the composite. The failure of the LAS matrix to protect the fibers poses a severe limitation for the application of this system at higher temperatures.

Concluding Remarks

What is remarkable about these composites, when compared with monolithic ceramics, is the narrowoness of their strength distribution as measured by the MCS. The presence of the fibers appears to play an important role in narrowing the distribution and limiting the size of the initial flaws. In general, unless the surface was badly damaged, it is reasonable to assume that the size of the prexisting flaw sizes would be limited to the interfiber spacing.

By measuring the the electrical resistance changes of a thin gold film sputtered on the surface of the composite as a function of applied stress in three point bend tests it is possible to accurately and unambigously measure the MCS in fiber reinforced ceramic composites. The advantages of this technique are several and include:

i) The ease by which the MCS can be unambigously determined, even for low fiber volume fractions.

ii) Once gold coated post-test examaination of the damaged surface is readily carried out

iii) The technique can differentiate between various types of cracks such as individual fibers breaking, matrix cracks or cracks parallel to the fibers.

The MCS for a 50 v% SiC Nicalon-LAS composite was found to be 370± 10 MPa. This value was not a strong function of mild HF etching. Heating in air for 24 hrs at 1000 °C resulted in a brittle layer forming on the surface, that cracked easily upon application of the load. The MCS for a 43v% C/corosilicate matrix composite was measured to be 360±MPa. Mild etching (120s in 5 %HF) almost doubled the MCS to over 650 MPa.

AKNOWLEDGEMENTS

The author thanks Dr. S. Freiman, NIST, for supplying the samples and for many

illuminating and helpful discussions and especially for pointing out the importance of polishing prior to testing. The author would also like to thank Mr. Scott Holder of Drexel University for carrying out some of the resistance measurements. The discussions with Prof. A. Wang of Drexel University and Dr. K. Prewo of UTRC have also been very valuable.

Supported By: National Bureau of Standards, under contract No.41-USC-252-C3 and the Air Force Office of Scientific Research under contract # AFOSR-88-0113.

APPENDIX

In their as-recieved condition the samples had a thin glassy film on their surface. A typical response of a gold film on such a surface is shown in Fig. A1 (lower right hand side). The glassy layer was found to crack at very low stresses and mask the response of the underlying matrix, hence the need for polishing prior to applying the gold film. Also shown in Fig. A1 is the response of the oxidized sample.

Polishing, without mounting resulted in the three region response shown in Fig. 3. In region II, the resistance changes observed at maximum stress are not recovered when that stress is removed (see Figs. 3) indicating that the cracks that caused the damage do not close. When the tests where interrupted in this region the only types of cracks that were visible in the SEM, even when observed without load, were those associated with broken fibers it follows that the damage in region II has to be associated with individual fiber breaks.

The extent of fiber damage, as measured by $\Delta R_{max}/R_o$ just prior to the matrix cracking varied from not being present (Fig. 2) to almost 0.1. The MCS, however, was not affected.

Polishing using the sample holder reduced fiber damage significantly and, as a result, data similar to the curves shown in Fig. 2, where region II is absent, are now routinely generated. It should be pointed put that in the absence of region II there is no need to cycle the stress in order to determine the MCS since the response is quite sharp. The enhancement in the determination of the MCS when can be easily seen by comparing $\Delta R_{max}/R_o$ (Fig. 3) to the curves shown in Fig. 4. Subtracting the baseline associated with fiber breaks clearly enhances the accuracy by which the MCS can be determined.

REFERENCES

1) K . Prewo, "Fatigue and Stress Rupture of SiC Fiber-Reinforced Glass-Ceramics", J. Mater. Sci. **22**, (1987) pp.2695-2701.

2) T. Mah, M.G. Mendiratta, A.P. Katz, R.Ruh & K.S. Mazdiyasni, " Room-Temperature Mechanical Behavior of Fiber-Reinforced Ceramic-Matrix Composites", J. Amer. Cer. Soc. **68**, C-27-C30 (1985).

3) D.B. Marshall and A.G. Evans, " Failure Mechanisms in Ceramic-Fiber/Ceramic-Matrix Composites", J. Amer. Cer. Soc., **68,** pp.225-231, (1985).

4) K. Prewo, "Tension and Flexural Strength of Silicon Carbide Fiber Reinforced Glass Ceramics", J. Mat. Sci., **21**, (1986) pp.3590-3600.

5) K.M. Prewo, " Carbon Fiber Reinforced Glass Matrix Composite Tension and Flexure Properties", J. Mat. Sci., **23**, (1988) pp.2745.

6) V.C. Nardone & K.M. Prewo, " Tensile Performance of Carbon-Reinforced Glass", J. Mat. Sci., **23**, (1988) pp.168-180.

7) R.Y. Kim & J. Pagano, "Initiation of Damage in Unidirectional Brittle Matrix Composites", to be published in Proceedings of 4th U.S./Japan Conf., Wash, D.C..

8) M. Barsoum & O. Zhou, "Microcracking in Ceramic/Ceramic Composites", Adv. Cer. Materials, **3**, pp.361-68, (1988).

9) J. Aveston, G.A. Cooper & A. Kelly, " Single and Multiple Fracture Fracture" in The Properties of Fiber Composites, Conf. Proc. pp.15-26 National Physical Laboratory, IPC, Science and Technology Press (1971) .

10) D.B. Marshall, B.N. Cox and A.G. Evans, " The Mechanics of Matrix Cracking in Brittle-matrix Fiber composites", Acta Met., **33**, pp.2013-2021 (1985).

11) L.N. McCartney, " Mechanics of Matrix Cracking in Brittle Matrix Fiber-Reinforced Composites", Proc. R. Soc. [illegible] **A 409**, pp.329-350 (1987).

12) W. Haller, U. Deshmukh & S. Freiman, " Novel Process for the Preparation of Fiber-Reinforced Ceramic-Matrix Composites", To be published in J. Amer. Cer. Soc.

13) J. Chou, M.Barsoum and M.J. Koczak. In preparation.

14) T. Mah, M.G. Mendiratta, A.P. Katz, R.Ruh & K.S. Mazdiyasni, " High-Temperature Mechanical Behavior of Fiber-Reinforced Glass-Ceramic-Matrix Composites", J. Amer. Cer. Soc. **68**, C-248-C251 (1985).

15) K. Prewo & J. Brennan, " High Strength Silicon Carbide Fiber-Reinforced Glass-Matrix Composites", J. Mat. Sci. , **15**, pp.463-468 (1980).

TABLE 1: Summary of matrix cracking stresses for SiC and C fiber reinforced glass and glass ceramic matrices.

System	V_f	MCS (MPa)	Comments	Ref.
SiC‡ -LAS	0.5	290±20	In situ observation of matrix crack formation in tension and flexure	3
SiC‡ -LAS*	0.4	300	Tension	2
	0.4	550	Flexure	2
SiC‡ -LAS II	0.46	381	Tension, as pressed	4
		439	Tension, ceramed	4
	0.44	345	Tension, as pressed	4
	0.44	391	Tension, ceramed	4
SiC‡ -LAS	0.4	300-565	4-point flexure	1
	0.40	270	Tension	1
SiC‡ -LAS	0.5	370±10	3 and 4-point flexure	This work
C$ - boro-silicate#	0.29	50	Tensile (average 2 samples)	5
	0.35	182	"	5
	0.40	293	"	5
	0.43	290	Tensile (average 3 samples)	6
	0.43	360±2	3 point flexure (2 samples)	This work
	0.55	476	Tensile (average 2 samples)	5

‡Nicalon * Corning Code 9608 # Corning Code 7740 $ Hercules HMU carbon fiber

Table 2: Summary of properties of composite systems.

	SiC‡/LAS ¶	SiC*/Borosilicate#	C*/Borosilicate#
K_c^m	2 MPa √m	0.75 MPa√m	0.75 MPa √m
E_f	200 GPa	400 GPa	380
E_m	85 GPa	63 GPa	63
V_f	0.5	0.17	0.45
R	8 μm	70 μm	4 μm
τ	2 MPa	10 MPa (Ref. 13)	25 MPa (Ref. 5) 10 MPa (Ref. 10)
Calculated MCS σ_o [Eq. 2]	270 MPa	66 MPa	792 MPa for τ=25 584 MPa for τ=10
Measured MCS	370 ±10 MPa	78 ±10 MPa	360±2 MPa

‡ Nicalon ¶ Data taken from Ref. 10. * SCS-6 AVCO fibers
# Corning Glass Works, Type 7740 * HMU type (Hercules Co.)

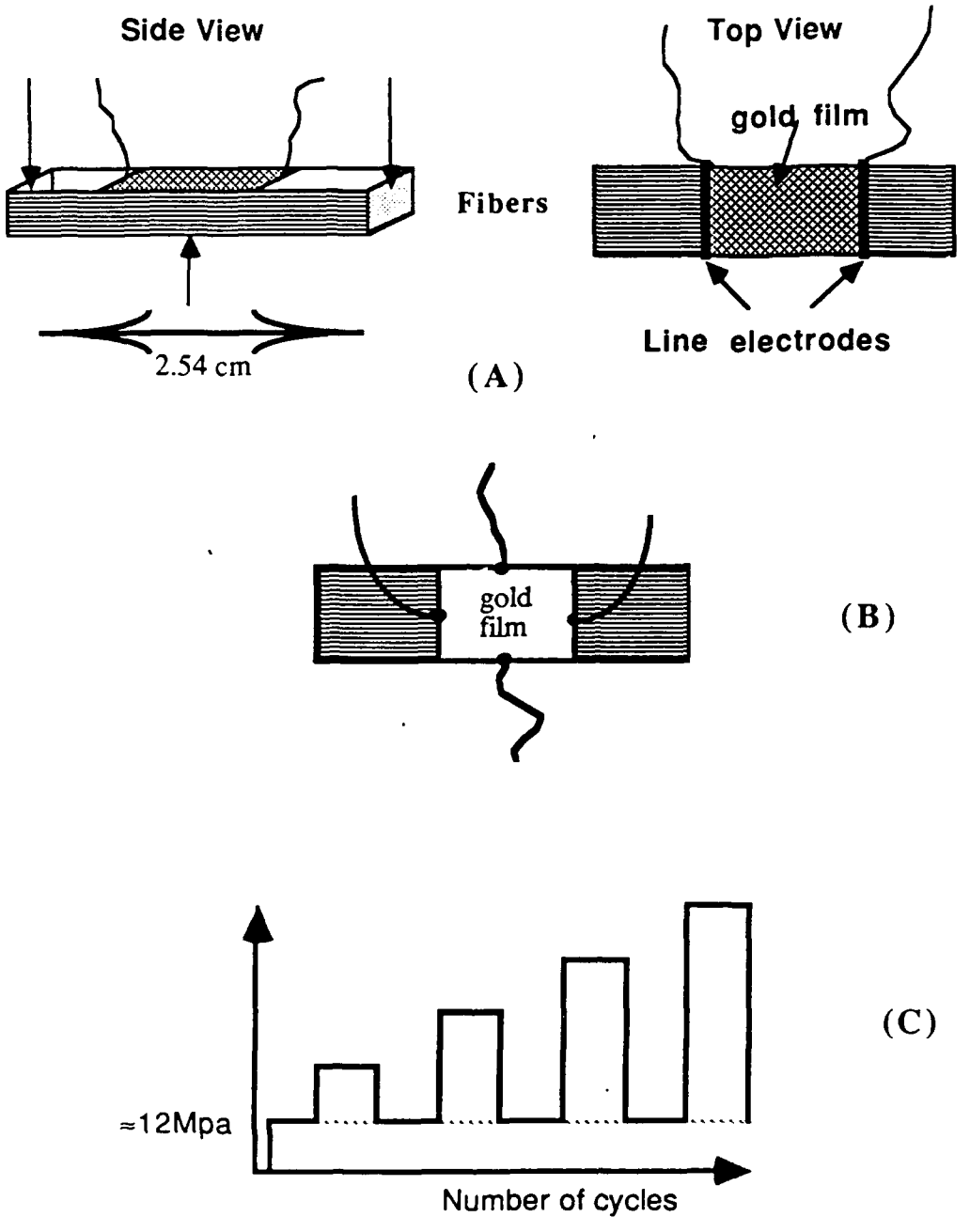

Figure 1: Experimental setup. a) Relationship between fibers, line electrodes and applied load.b) 4-Point electrodes. c) Loading cycles. The load was never totally removed. The resistance was measured at maximum and minmum loads.

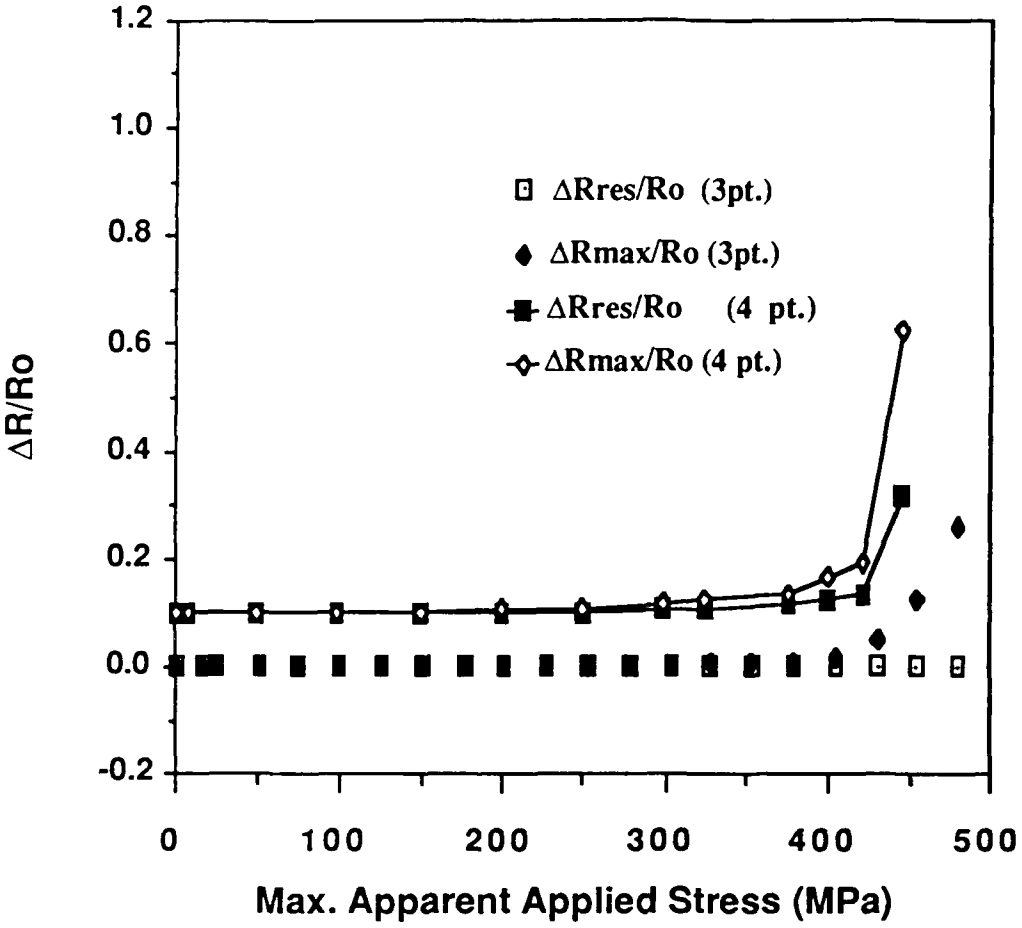
1.2
1.0
0.8
0.6
0.4
0.2
0.0
-0.2
ΔR/Ro
ΔRres/Ro (3pt.)
ΔRmax/Ro (3pt.)
ΔRres/Ro (4 pt.)
ΔRmax/Ro (4 pt.)
0
100
200
300
400
500
Max. Apparent Applied Stress (MPa)

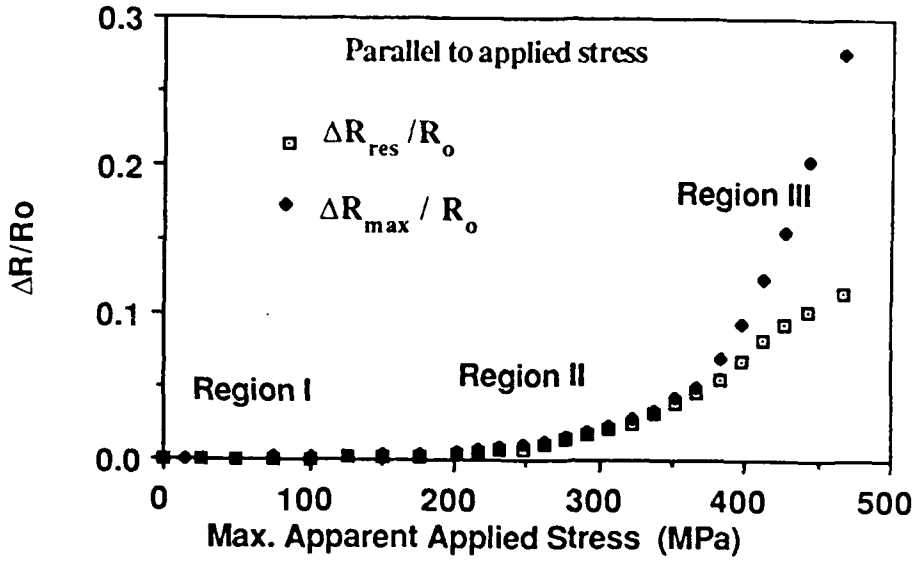
Parallel to applied stress
$\Delta R_{res}/R_o$
$\Delta R_{max}/R_o$
Region I
Region II
Region III
ΔR/Ro
0.0
0.1
0.2
0.3
0
100
200
300
400
500
Max. Apparent Applied Stress (MPa)

(A)

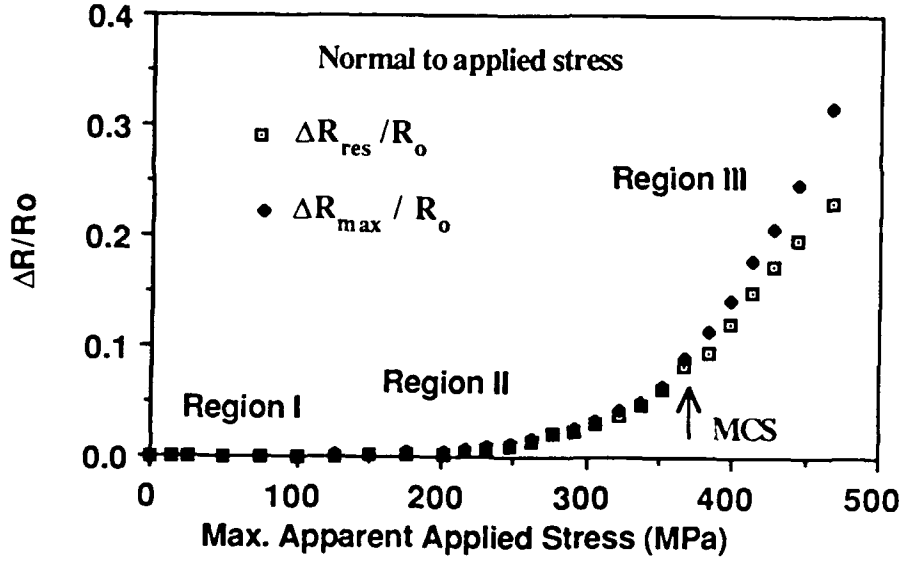
Normal to applied stress
$\Delta R_{res}/R_o$
$\Delta R_{max}/R_o$
Region I
Region II
Region III
MCS
ΔR/Ro
0.0
0.1
0.2
0.3
0.4
0
100
200
300
400
500
Max. Apparent Applied Stress (MPa)

(B)

Figure –

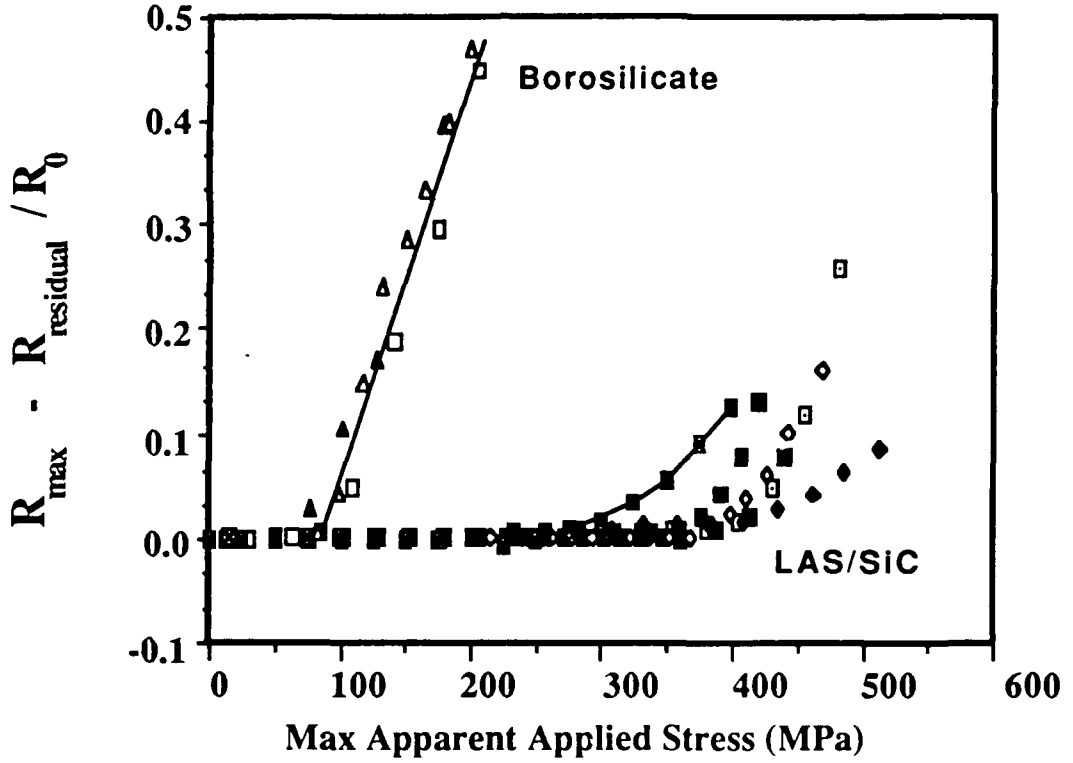
0.5
0.4
0.3
0.2
0.1
0.0
-0.1
0
100
200
300
400
500
600
Borosilicate
LAS/SiC
R_{max} - $R_{residual}$ / R_0
Max Apparent Applied Stress (MPa)

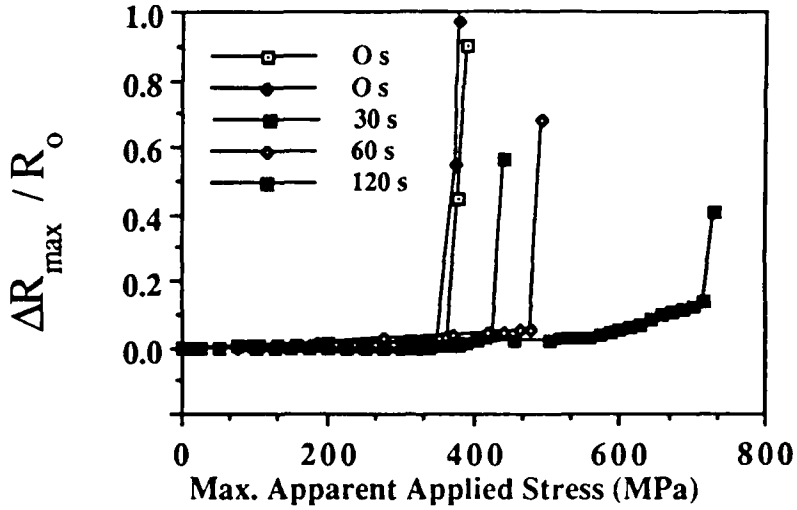
1.0
0.8
0.6
0.4
0.2
0.0
$\Delta R_{max} / R_o$
0 s
0 s
30 s
60 s
120 s
0
200
400
600
800
Max. Apparent Applied Stress (MPa)

(A)

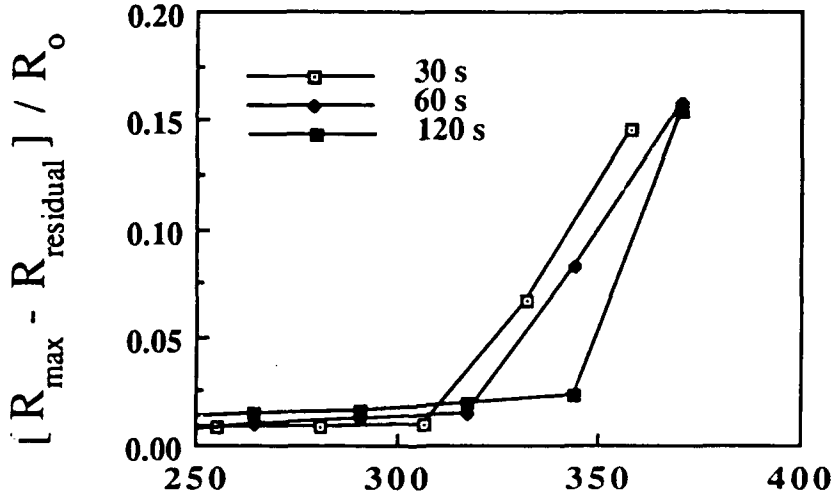
0.20
0.15
0.10
0.05
0.00
$[R_{max} - R_{residual}] / R_o$
30 s
60 s
120 s
250
300
350
400
Max. Apparent Applied Stress
(MPa)

(B)

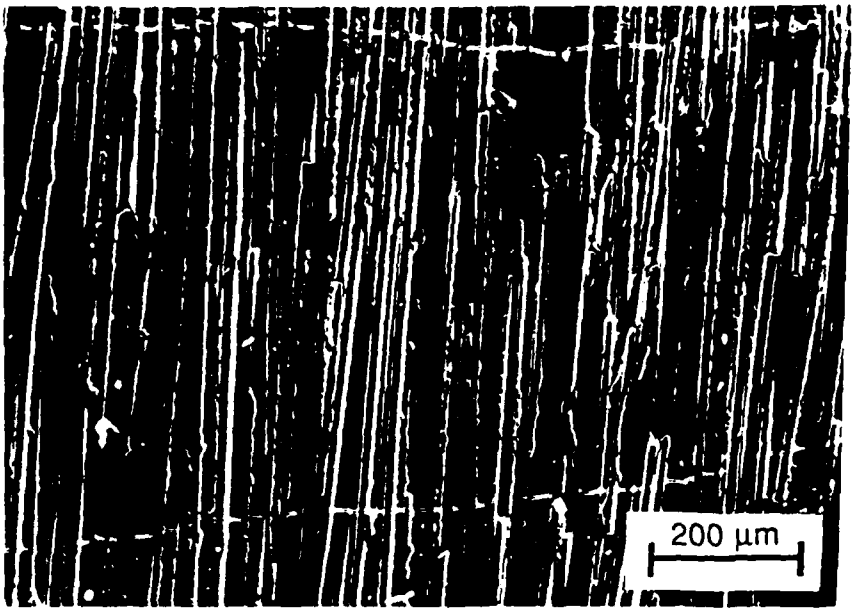

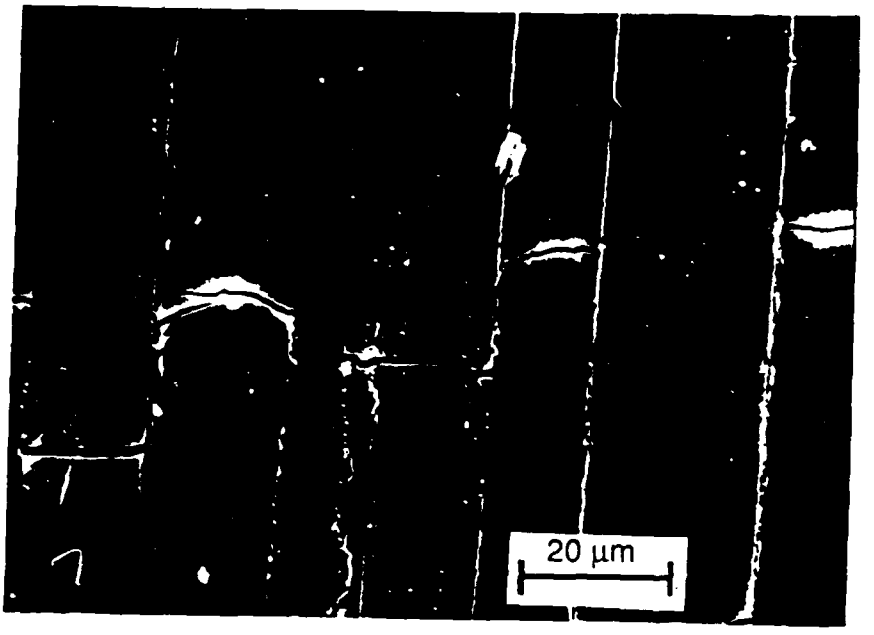

Fig 3

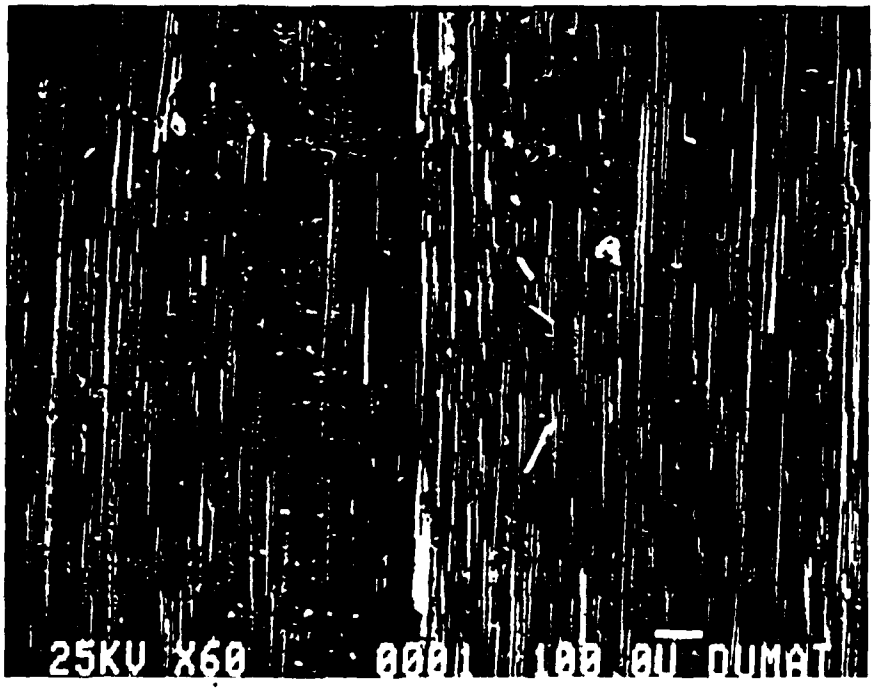

Fig. 7

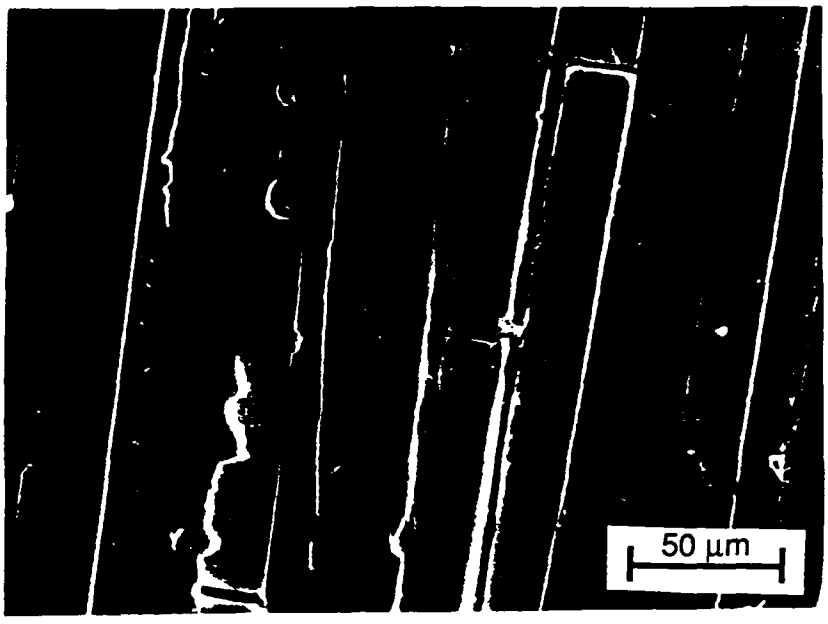

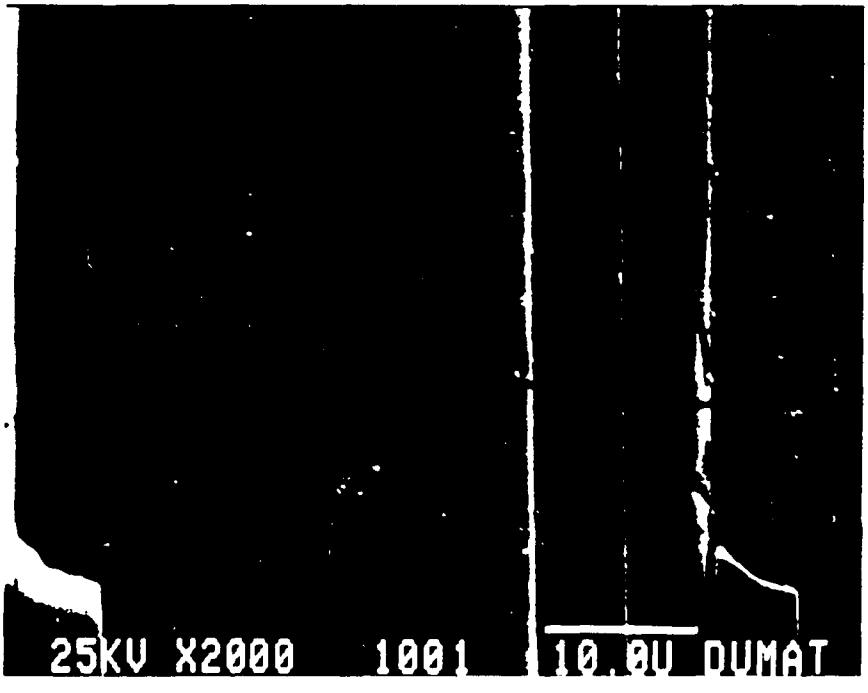

Fig. 3

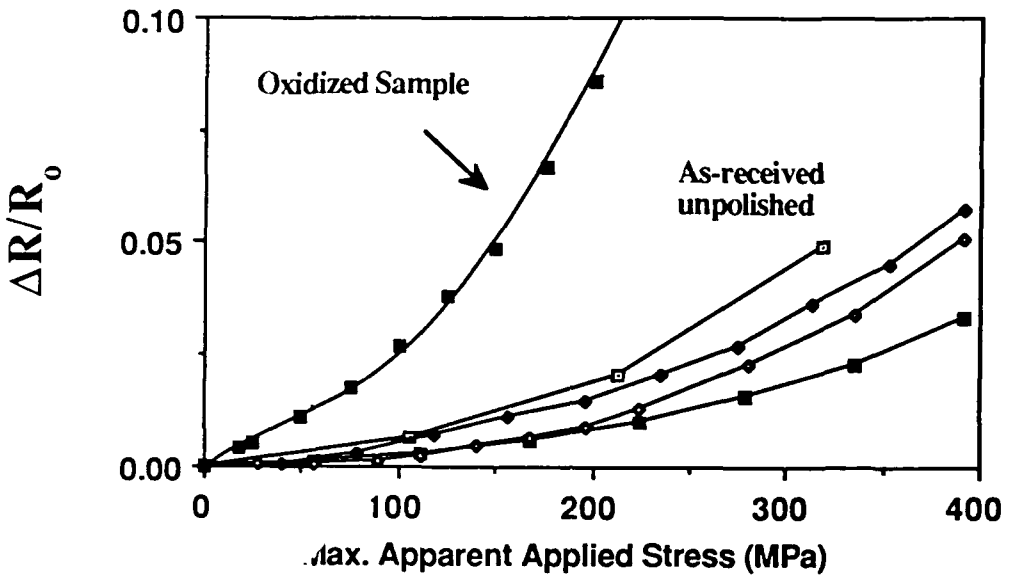

APPENDIX FIGURE A1

MATRIX CRACKING INITIATION IN BRITTLE-MATRIX COMPOSITES

A. S. D. Wang, Michel W. Barsoum and X. G. Huang
Drexel University
Philadelphia, Pa. 19104

ABSTRACT

This paper discusses the mechanics of matrix crack initiation in unidirectionally fiber-reinforced ceramic-matrix composites loaded in axial tension. Several models that predict the matrix crack initiation stress (MCIS) are first reviewed, with emphasis placed on the physical parameters involved in the models. Then, in an effort to study the influence of these parameters on the MCIS, specimens made of SiC/LAS with 50% fiber-volume content, SiC/Borosilicate with 17% fiber-volume content, and C/Borosilicate with 40% and 45% fiber-volume content are tested under three-point bending.

To measure the MCIS, the surface of the tensile side of the specimens is sputtered with a thin gold-film prior to loading; and the electrical resistance of the gold-film is monitored during loading. When matrix cracking is initiated on the tensile surface of the specimen, the gold-film cracks with the substrate material and causes a sudden increase in the film's resistance. This technique determines the MCIS in real-time and provides a load-history of matrix cracking beneath the gold-film.

A comparison is made between the experimentally measured MCIS and those predicted by two principal matrix cracking models.

INTRODUCTION

When a unidirectionally fiber-reinforced ceramic matrix composite is loaded in tension in the fiber direction, matrix cracks normal to the fibers are often induced at very low strains with the fibers still remaining intact. This type of fracture occurs because the matrix material is more brittle than the reinforcing fibers. To improve the fracture and

toughness performance of such composite systems, there have been numerous studies aimed at understanding the basic mechanisms of this type of matrix cracking.

Aveston, Cooper and Kelly [1] followed a micromechanics analysis approach and formulated a closed-form expression for the critical composite stress at the initiation of matrix cracking:

$$(\sigma_c)_{cr} = E_c \{[\, 12\, \gamma_m\, \tau\, E_f\, (V_f)^2] / [\, E_c\, E_m^2\, V_m\, R\,]\}^{1/3} \qquad (1)$$

where γ_m is the surface energy density of the matrix; E_m, E_f and E_c are the moduli of elasticity of the matrix, fiber and composite (in the fiber direction), respectively; R is the fiber diameter; V_m and V_f are the matrix and fiber volume-content, respectively; and τ is the fiber-matrix interface shear strength.

The ACK model, Eq. (1), contains three independent constituent material variables (E_m, E_f and γ_m), two independent geometric variables (R and V_f) and a fiber-matrix interface property defined as the fiber-matrix interface shear strength, τ.

Fig. 1 shows the physical features of the ACK model. Here, it is assumed that a fiber-bridged matrix crack of sufficient length already exists, and it is propagating steadily across the fibers. The fibers that bridge the crack are assumed to pull out of the matrix uniformly so that crack opening in the wake of the crack approaches an equilibrium separation (this idealized cracking mode has been referred to as steady-state matrix crack propagation [2,3]). In such a state, the driving force at the crack-tip can be assumed to be independent of the crack size; hence an energy balance equation can be written, per unit length of crack extension, as follows:

$$\Delta W_\sigma + \Delta U_m = 2\gamma_m V_m + W_d + W_s + \Delta U_f \qquad (2)$$

where the energy terms are, respectively, the work done by the far-field applied tensile stress, the strain energy released by the cracked matrix, the matrix fracture surface energy, work done in debonding the fiber-matrix interface, frictional work as fibers slide against the matrix, and the strain energy stored in the bridging fibers.

The actual expression and the value of each of the energy terms may vary depending on the manner in which they are evaluated. ACK [1], for instance, evaluated each term by an approximate, one-dimensional analysis treating the fiber and the matrix as two distinct elastic materials. The closed-form expression in Eq. (1) is obtained when the work done in interface debonding (W_d) and frictional sliding (W_s) is combined as the work done in overcoming the interface shearing resistance represented by τ. The latter is assumed a property of the fiber-matrix interface which can be characterized, for instance, by pushing a fiber into or pulling a fiber out of the matrix.

Marshall, Cox and Evans [2] and McCartney [4] each extended the ACK model by allowing the initial matrix crack to have an arbitrarily small size. The problem is treated as a fracture mechanics problem involving mode-I crack propagation in a two-dimensional effective homogeneous medium, instead of a discrete fiber-matrix composite medium. Here, the effect of fiber-bridging in the wake of the crack is represented by an equivalent surface traction distributed normal to the crack surface, with the traction accounting for the debonding and/or the frictional sliding of the fiber-matrix interface. Mode-I stress intensity factor K_1 at the crack-tip is then calculated; and the propagation of the initial matrix crack is determined by the composite's critical stress intensity factor K_{1c}.

The MCE and the McCartney models differ principally in their representation of the equivalent crack-surface traction and the definition of the stress intensity factor K_{1c} of the composite. The MCE model, however, provides a closed-form expression for the critical composite stress, σ_c, required to propagate the matrix crack of small size, a:

$$(\sigma_c / \sigma_m) = (1/3)\,(a / c_m)^{-1/2} + (2/3)\,(a / c_m)^{1/4} \qquad (3)$$

where c_m is a characteristic length defined as:

$$c_m = (\pi K_{1c} / \alpha I^2)^{2/3} \qquad (4)$$

and σ_m is a characteristic stress defined as

$$\sigma_m = (3/\sqrt{\pi}) (K_{1c}^2 \alpha I^2)^{2/3} \quad (5)$$

Expressions (4) and (5) contain several material and geometrical variables implicit in the definition of

$$K_{1c} = K_m E_c / E_m \quad (6)$$

and

$$\alpha = [8(1- \nu^2) \tau V_f^2 E_f] / [E_m V_m R \pi^{1/2}] \quad (7)$$

where K_m is the mode-I critical stress intensity factor of the matrix (= $\sqrt{(2\gamma_m E_m}$ for generalized plane stress), I is a dimensionless crack geometry constant (=1.2 for a straight crack) and ν is the composite Poisson Ratio transverse to the fibers.

Eq. (3) is a non-dimensional (universal) relation between (σ_c/σ_m) and (a/c_m); it is valid for matrix cracks having initial size $a < c_m/3$. In this range, the critical composite stress σ_c is roughly proportional to $(a)^{-1/2}$. For cracks having a size larger than $c_m/3$, the critical stress can be shown to approach the value given by ACK, Eq. (1).

McCartney [4], on the other hand, defines the characteristic length (denoted by a_o) as

$$a_o = (\sqrt{\pi} K_{1c} / \lambda^2)^{2/3} \quad (8)$$

and the characteristic stress σ_o as

$$\sigma_o = (K_{1c}/\sqrt{(\pi a_o)} \quad (9)$$

A non-dimensional (universal) relation between (σ_c/σ_o) and (a/a_o) is obtained and expressed as

$$\sigma_c / \sigma_o = [\mu_c Y^2 (\mu_c)]^{-1/3} \quad (10)$$

where $Y(\mu_c)$ is a complicated integral equation involving μ_c which is defined as

$$\mu_c = (\lambda^2 a) / (\pi \sigma_c) \quad (11)$$

with

$$\lambda = 2(V_f/V_m)(2\pi \tau E_f E_c/R E_m^2)^{1/2} \quad (12)$$

and

$$K_{1c} = (V_m E_c/E_m]^{1/2} K_m \quad (13)$$

The McCartney relation in Eq. (10) is valid for matrix crack of any initial size. However, a numerical procedure is required to calculate the a versus σ_c relation from Eq. (10) for any given composite system. Generally, the McCartney model differs somewhat from the MCE model in the region of small crack size. But for matrix crack of large initial length, Eq. (10) also reduces to the ACK model as expressed in Eq. (1).

These short crack models are essentially derivatives of the ACK model as they are based on the same matrix crack initiation mechanisms as represented by Fig. 1. Furthermore, these models involve the same micromechanical variables as in the ACK model, except for the inclusion of the crack size effect, and a 2-dimensional effect which is reflected by the composite Poisson ratio, ν, through Eq. (7).

To use either the MCE or the McCartney model to predict the MCIS, a knowledge of the initial matrix crack size a is needed. In either case, the predicted MCIS varies essentially with the inverse of $\sqrt{a}$ for small cracks; thus it is sensitive to the accuracy of the measurement of the initial crack size. The ACK model, Eq. (1), on the other hand, predicts a constant MCIS for relatively large cracks and is the lower-bound for the two short crack models. Thus, in practice, the ACK model can be used to estimate the minimum possible MCIS.

A different rationale on how matrix cracking is initiated has recently been taken by Wang [5]. This rationale is based on the assertion that composites inherently contain

distributed microflaws. In fact, the microflaws exist randomly both in the interior and on the surface of the composite. Matrix cracking is then theorized as being initiated either from a single critical flaw or from a cluster of mutually interacting flaws. To implement this rationale into a mechanistic modeling scheme, however, both the physical identity and the mathematical representation of the distributed flaws will be necessary. If this is to be done in the true sense of the word, it would clearly be a practically impossible task.

To circumvent this difficulty, the concept of effective flaws proposed earlier by Wang [6] is employed. In this concept, the composite is assumed to contain randomly distributed "effective" flaws whose identity and distribution are simply presumed known, see Fig. 2a. Then, under a certain loading condition, some dominant microflaw or a cluster of such flaws will become critical and initiate matrix cracking on the macroscale. The critical condition is provided by a certain fracture criterion.

Specifically, to model the fiber-bridged matrix cracking problem discussed above, two kinds of effective flaws will be assumed to exist. Namely, flaws in the matrix material and flaws in the fiber-matrix interface, as shown schematically in Fig. 2b. Of course, these effective flaws are merely hypothetical in nature; their presence in terms of shape, size and location will have to be assumed at this time. The flaws and the matrix-fiber geometry then constitute the microstructure of the composite at a specific location. And, this knowledge enables the construction of a mechanics model that mimics the postulated matrix crack initiation mechanisms.

Fig. 3 identifies this local microstructural cell, which is assumed a probable matrix crack initiator. Here, a flaw of size a is situated in the matrix between two fibers and a pair of interfacial flaws, each of size 2b, are flanking the matrix flaw. The matrix flaw is then assumed to act like a small crack, which will propagate at some critically applied composite tension. The presence of the interfacial flaws can influence the criticality and the character of the matrix flaw propagation, depending on the geometrical layout of the cell. Matrix crack initiation on the macroscale is defined when this matrix flaw propagates and links with the interfacial flaws.

The latter is described mathematically by the method of fracture mechanics, in conjunction with a quasi-three-dimensional finite element crack-closure procedure [6].

Specifically, the strain energy release rate at the tips of the matrix flaw, Fig. 3, is numerically calculated and expressible in the form:

$$G(e_c, \Delta T, a, b) = [\sqrt{C_e}(a,b)\, e_c + \sqrt{C_T}(a,b)\, \Delta T]^2 d \qquad (14)$$

where e_c is the applied composite tensile strain, ΔT is a temperature load residing in the composite due to fabrication, and $C_e(a,b)$ and $C_T(a,b)$ are computed coefficient functions for the energy release rate due to the application of e_c and ΔT, respectively. These functions depend implicitly on the quantities a and b, the elastic constants of the fiber and matrix, and the spacing between fibers, t (see [5] for details).

The critical condition for matrix crack initiation is provided by the fracture mechanics criterion:

$$G(e_c, \Delta T, a, b) = G_m \qquad (15)$$

where G_m $(=2\gamma_m)$ is the critical strain energy release rate of the matrix.

The critical composite strain e_c is determined from Eq. (15); and the critical composite stress or the MCIS is given by:

$$\sigma_c = E_c\, e_c \qquad (16)$$

It is noted that the rationale taken in the flaw-interaction model differs from that in the ACK model. In particular, the flaw-interaction unit-cell (Fig. 3) is endowed with a microstructure that allows a direct simulation of matrix crack initiation at the fiber-matrix level. To apply the flaw-interaction model to specific problems will require the knowledge of the distributed effective flaws. As it will be shown in the reminder of this paper, this can be achieved in conjunction with some heuristic arguments of an empirical nature. Here, a statistical range of the distributed effective flaws is first estimated and the corresponding range of the MCIS is then established. These results are ultimately compared with the experiment.

EXPERIMENT AND RESULTS

In this section, we shall present some experimental data of matrix cracking initiation stress from specimens tested under 3-point bending. In the experiment, an effort is made to study the influence of some of the micromechanics variables on the MCIS. Several composites, having different material combination and/or microstructural variations, were fabricated and tested. The ACK and the flaw-interaction models discussed previously are then applied to provide a prediction for the MCIS in each case.

Three composites systems are selected in the test. These are the SiC/LAS system with 50 v% (Nicalon) fiber, SiC/Borosilicate system with 17 v% (AVCO) fiber and the C/Borosilicate system. The latter was fabricated with 40% and 45 v% (HMU graphite) fibers. The fabrication processes for these composites and the preparation details of the test specimens have been described elsewhere [7]; the relevant constituents and composite properties in each system are either characterized by tests or gathered from known sources. Table 1 is a list of these properties.

It is noted from Table 1 that these composite systems provide a range of variations for some of the most important micromechanics parameters. Specifically, we note the variations in the fiber stiffness E_f (200, 380, 400 GPa), in the fiber diameter d (8, 16, 140μm), in the fracture toughness of the matrix K_m (0.75, 2 MPa$\sqrt{m}$), in the fiber-volume fraction V_f (0.17, 0.4, 0.45, 0.5), in the thermal expansion mismatch α_m-α_f (0.6, 1, 3.1 x10^{-6}/^{o}C), and in the interfacial shear strength τ, obtained from single fiber pull out tests, (2, 10, 25 MPa).

The 3-point bend test specimens are prepared in the form of flat bars whose length-width-depth dimensions ranged 3x0.5x0.18 cm for the SiC/LAS, 3x0.5x0.2 cm for the SiC/ Borosilicate and 3x0.5x0.44 cm for the C/Borosilicate. The lower pin-supports span 2.54 cm; all tests are conducted at room temperature.

The tensile surface of each bar is first polished down to 0.05 μm using alumina powder (Linde B) to remove any glassy layers due to fabrication. A 1000 nm thick gold

film is then sputtered on the polished surface; and a pair of line electrodes normal to the fibers are attached to the gold film using a conductive epoxy paste, Fig. 4a. The initial electrical resistance of the gold film, R_o, is measured using a digital multimeter

The load is applied using a manually operated tester and the maximum composite stress on the tensile surface of the bar is computed assuming a simple elastic beam in 3-point bending. For reasons that are discussed in more details in [7], a sequence of step-loads is applied, as shown in Fig. 4b. In each step-load cycle, the resistance of the film, R_{max}, is measured at the peak load; and the residual resistance, R_{res}, is measured when the load is lowered to an equivalent of about 12 MPa bending stress on the tensile surface. In the next cycle, the peak load is taken to a higher value and then lowered, with the corresponding resistances of the film measured. A plot of $(R_{max} - R_{res})/R_o$ versus the applied maximum composite surface stress is obtained in each specimen so tested.

Fig. 5 shows the experimental plot from four specimens of the SiC/ LAS system. It is seen that the value of $(R_{max} - R_{res})/R_o$ increases dramatically when the applied composite stress reaches a certain critical value. Correlation with SEM examination of the tested specimen proves that matrix cracks are initiated at this critical stress level [7]. The MCIS for the SiC/LAS specimens is thus determined from the plot to be 370±10 MPa.

Similarly, Fig. 6 shows the plot for two SiC/Borosilicate specimens. The MCIS determined from this plot has a range of 65±5 MPa. The corresponding plots for the C/Borosilicate specimens of 40% and 45% fiber contents are shown in Figs. 7 and 8, and their respective MCIS ranges are found to be 320±20 and 360±2 MPa.

The experimental MCIS ranges are listed in Table 2, along with their counterparts predicted by the ACK model and the flaw-interaction model.

PREDICTED MATRIX CRACK INITIATION STRESS AND BOUNDS

As has been discussed previously, the ACK model provides the lower bound value of MCIS for matrix cracking in the mode shown in Fig. 1. This lower bound value is found for each of the material systems tested by means of Eq. (1), along with the relevant parameters listed in Table 1. It should be noted that the reported values of the interface

shear strength, τ, for the C/borosilicate system range from 10 to 25 MPa. Since the MCIS scales with $\tau^{1/3}$ in the ACK model, this causes a wide range of the predicted values.

Table 2 lists the various computed MCIS values for specimens made of SiC/LAS, SiC/borosilicate, C/Borosilicate of 40 v% fiber content and C/Borosilicate of 45 v% fiber content as they are compared with the experimental MCIS. It is seen that the ACK model predicted well for the SiC/Borosilicate specimens, but under predicted for the SiC/LAS specimens and over predicted for the C/Borosilicate specimens, although in theory the ACK prediction is the lower bound of MCIS.

In view of the sensitivity of the model on several parameters whose actual values are uncertain (e.g. τ) and the fact that the present experimental data is limited, caution should be taken when a comparison is made of the results listed in Table 2.

Now, if the MCE and/or the McCartney models are to be used, then the initial matrix crack size c (for MCE) or a (for McCartney) must be specified a priori. In this regard, the respective characteristic length c_m and/or a_o must be calculated in order to determine whether the initial matrix crack is short or long. Note that in the MCE model, a matrix crack is considered long if $c > c_m/3$; while in the McCartney model, a long crack is when $a > 5a_o$.

For the SiC/LAS system, the calculated c_m is 325μm and a_o is 26μm. Thus, an initial matrix crack of 110μm ($c_m/3$) or 130μm ($5a_o$) would be considered a long crack by the respective models. Since the diameter of the SiC fibers (Nicalon) is on the order of 16μm, a long crack would be on the order of 6 to 8 fiber diameters according to these models. On the other hand, for the SiC/Borosilicate system, the calculated c_m and a_o are 817μm and 94μm, respectively; thus, a long crack would be one which is longer than 270μm or 470 μm depending on the model. In this case, the fiber diameter is 140μm so that an initial crack of 2 to 3 fiber diameter is considered already long. As for the C/Borosilicate system (e.g. 45 v%), the calculated c_m and a_o are 37μm and 1.6μm. A long

crack would be in the order of 12μm and 8μm, respectively, while the carbon fiber diameter in this system is 8μm.

From these calculations, it seems that the classification of a short or a long crack does not bear any physical implication. In any event, one cannot apply any of the short crack models until the initial crack size is measured precisely.

Next, we apply the flaw-interaction model, the schematic of which is depicted in Fig. 3. We define the MCIS as the critical stress at the propagation of the matrix flaw of size a by the fracture criterion, Eq. (15). To do so, calculation of the strain energy release rate $G(e_c,\Delta T)$ for the various composite systems must be carried out by the finite element procedure using the appropriate material constants given in Table 1. Referring to the expression of $G(e_c,\Delta T)$ in Eq. (14), only the coefficients $C_e(a,b)$ and $C_T(a,b)$ need to be calculated. In this regard, these coefficients are calculated by treating the matrix flaw size a as a variable while the interfacial flaw size b as a parameter.

Fig. 9a and 9b show, respectively, the coefficients $C_e(a,b)$ and $C_T(a,b)$ for the SiC/LAS system. Note that the range of a is taken from 0 to 1d, while the interfacial flaw size is taken with the values of b = 0, 0.2, 0.5, 0.75 and 1d. Here, it is assumed that the matrix flaw resides between two adjacent fibers; thus, its size is limited by the fiber spacing t. For the SiC/LAS system of 50% fiber volume content, the average fiber spacing is on the order of $t \approx d$. With d=16μm (Nicalon SiC), this translates to a maximum possible matrix flaw size up to about 15μm.

As for the values of b, it is seen that when b=0, meaning perfect interface bonding, the associated energy curve first increases linearly with a, then reaches a maximum value at about a = 0.8d and eventually turns downward towards the fiber-matrix interface. This down-turn is caused by the fiber constraint, and in this case, the effect of fiber constraint is most effective due to good interface bonding. If the presence of interfacial flaws is assumed, then $b > 0$. Depending on the size of b, the effect of fiber constraint is more or less reduced and the available energy release rate increases correspondingly. In this case, it is seen that fiber constraint is lost completely when the interfacial flaw size is on

the order of b=d. Thus, the effective range of b is from 0 to about 1d.

In this context, the energy release rate coefficients can then be used to determine the critical composite stress at the propagation of the matrix flaw if both the matrix flaw size a and the interface flaw size 2b can be estimated.

For the SiC/LAS system, we note from Table 1 that the experimental interfacial shear strength τ is of the order of 2 MPa. This value of τ is considered low, indicative of either a poor interfacial bonding, a low frictional sliding resistance or the presence of actual interfacial flaws. If perfect bonding is assumed for the system; then b=0. From Fig. 9, we determine the maximum possible values for C_e and C_T at $a \approx 0.85d$. Namely, C_e = 95 GJ/m^3 and C_T = 0.085 J/m^3/^{o}C^2. Using Eq. (15) in conjunction with $G_m = (2\gamma_m)$ = 47 J/m^3, the critical composite strain is calculated as $e_c = 4.43 \times 10^{-3}$. From the rule-of-mixture, the axial composite modulus is 143 GPa. Hence, the calculated MCIS is σ_c = 633 MPa according to Eq. (16). This MCIS is for the assumed flaw size and perfect bonding .

If we relax the interfacial bonding completely by letting b=d and take the values of C_e and C_T also at a = 0.85d, we have C_e = 209 GJ/m^3 and C_T = 0.18 J/m^3/^{o}C^2. The calculated critical composite strain is then $e_c = 2.64 \times 10^{-3}$ and the MCIS is σ_c = 377 MPa. This MCIS value is for the system with practically no interfacial bonding.

In this sense, an upper bound (633 MPa) and a lower bound (377 MPa) for MCIS are obtained. When compared to the experimental value of 370±10 MPa (see Table 2), one is inclined to say that the lower bond value of MCIS should be used since the system has a rather poor interfacial bonding.

For the SiC/Borosilicate system, the energy release rate coefficients C_e and C_T are shown in Fig. 10a and Fig. 10b, respectively. In this case, the fiber volume content is 17% and the fiber diameter is 140μm (AVCO SiC). This means that the average fiber spacing is on the order of $t \approx 600\mu m$. Theoretically, a matrix flaw of this size could exist in between two adjacent fibers. However, in the present study, monolithic Borosilicate 3-point bend specimens were also fabricated and tested with their tensile surfaces polished using

Linde A & B, 600 grit sand paper and diamond scratch, respectively, to introduced surface flaws of various severity. These specimen yielded fracture stresses at 130 MPa, 75 MPa and 55 MPa, respectively. Using the same effective flaw postulate and the Griffith fracture criterion, this translates to an effective flaw in the monolithic matrix material on the order of 20, 65 and 120 μm, with respect to the variously polished surfaces.

Based on this information, we assume that the worst matrix flaw size in the composite may be on the order of a ≈120μm, which is about 0.85 times the AVCO fiber diameter. By examining Fig. 10, we see that in the range of a << t, the values of C_e or C_T are not affected by the presence of any interfacial flaws. In other words, the MCIS is determined in this case solely by the effective matrix flaw size, a.

Consequently, if we assume for the composite the worst flaw (i.e. a ≈120μm), the energy release rate coefficients found from Fig. 10a and Fig. 10b are C_e = 90 GJ/m^3 and C_T = 0.04 J/m^3/$^oC^2$, respectively, regardless the value of b. Using G_m= 8.92 J/m^3 for the borosilicate matrix (see Table 1), the calculated critical composite strain is $e_c = 0.51 \times 10^{-3}$. With E_c = 120 GPa, σ_c = 61 MPa.

On the other hand, if the composite could be fabricated and polished with flaws of lesser severity, the predicted MCIS could be increased. In the limit that the composite could be polished as smoothly as the monolithic borosilicate bar, where the effective surface flaw is as small as 20μm, then the calculated σ_c is on the order of 150 MPa.

This again establishes a pair of possible bounds (61 to 150 MPa) for the predicted MCIS. Note that the experimental MCIS range in this case is 65±5 MPa (see Table 2), which is slightly higher than the lower bound value. This seems to suggest that in the processed composite the effective matrix flaw size is considerably larger than in the bulk borosilicate matrix even if the former is carefully polished.

Fig. 11a and Fig. 11b show the energy release rate coefficients C_e and C_T for the C/Borosilicate specimens with 40 v% fiber content, while Fig. 12a and 12b show the coefficients for specimens with 45 v% fiber contents. To use these figures, we note that the

carbon fibers have an extremely small diameter (d = 8μm); and the average fiber spacing is on the order of 1.5d and 1.2d, respectively. These are the limits for the worst possible matrix flaw sizes. In addition, we note that the fiber-matrix interfacial shear strength τ (Table 1) ranges from10 to 25 MPa. This is considered to be a relatively strong bond and it suggests that the size of the interfacial flaws should be relatively small.

Thus, if we assume perfect bonding and set b=0, we determine from Fig. 11 the maximum values for C_e and C_T in each case (which occur at a≈1.2d and a≈0.95d, respectively):

fiber content	max. C_e, 10^9 J/m^3	max. C_T, J/m^3/$^oC^2$
40 v%	96	0.98
45 v%	75	0.90

Based on the above, the respective critical composite strains are calculated as being 1.81×10^{-3} and 2.12×10^{-3}, respectively; and the corresponding MCIS values are 344 MPa and 436 MPa. These values may be considered as the upper bounds for the two cases.

If we relax slightly the interfacial bonding by letting b=0.1d, then the respective MCIS values are calculated at 337 and 376 MPa. Lower values for MCIS can still be obtained by letting b > 0.1d. In view of the relatively strong interface bonding, the values computed for b=0.1d should be taken. These are seen to compare well with the corresponding experimental values of 330±20 MPa and 360 ±2 MPa (see Table 2).

From the above four examples, we see that the flaw-interaction model can be used to estimate an upper and a lower bound for the MCIS in conjunction with some heuristic estimation procedure for the effective flaw sizes. Depending on the particular fiber-matrix microstructural details, the sensitivity of the estimated MCIS bounds may or may not be influenced simultaneously by the interfacial bonding and the size of the matrix flaw. The effective flaw concept seems plausible but requires further refinements if the concept is to be developed into a useful and rational model.

CONCLUSIONS

In this paper, we have reviewed some predictive models for the matrix cracking initiation stress (MCIS) in brittle ceramic matrix composites, especially the ACK model and the flaw-interaction model. The physical basis of each model is examined in detail, with the emphasis placed on the necessary input parameters required by each of the models. To illustrate the use of the models, 3-point bending specimens are made using composite systems with four distinct microstructural combinations. These are tested at room temperature to determine their matrix crack initiation stresses (MCIS).

A tentative comparison is made between the experimental and predicted MCIS for purpose of illustration only. The comparison is not meant to judge the relative adequacy of any of the models because of the limited test data. An experimental and analytical correlation, involving full scale parametric studies on the various influencing variables, is clearly necessary in order to further validate the theories.

ACKNOWLEDGMENTS

This work has been supported by the Air Force Office of Scientific Research through a research grant to Drexel University.

REFERENCE

1. Aveston, J., Cooper, G. and Kelly, A, "Single and Multiple Fracture," in The Properties of Fiber Composites, Conference Proceedings, National Physical Laboratory, Guildford, UK. IPC Science and Technology Press Ltd., 1971, pp. 15-26.

2. Marshall, D., Cox, B. and Evans, A.,"The Mechanics of Matrix Cracking in Brittle-Matrix Fiber Composites," Acta Metall., Vol. 33, 1985, pp. 2013-2021.

3. Budiansky, B., Hutchinson, J. W. and Evans, A. G., "Matrix Fracture in

Fiber-Reinforced Ceramics," J. Mech. Phys. Solids, Vol 34, 1986, pp. 167-189.

4. McCartney, L. N., "Mechanics of Matrix Cracking in Brittle-Matrix Fiber-reinforced Composites," Proc. Roy. Soc. London, A-409, 1987, pp. 329-350.

5. Wang, A. S. D., "On Fiber-Matrix Interface Bonding and Composite Toughness," Proc. of the 1st USSR-Symposium On Mechanics of Composite Materials, Riga, Latvian SSR, 1989.

6. Wang, A. S. D.,"Fracture Mechanics of Sublaminate Cracks in Composite Materials," Composite Technology Review, Vol. 6, 1984, pp. 45-62.

7. Barsoum, M. and Plotnick, B., "Matrix Cracking Stresses in Uniaxially Fiber Reinforced Ceramic Composites," (submitted for publication).

TABLE 1 SUMMARY OF PROPERTIES OF COMPOSITE SYSTEMS

	SiC+/LAS@	SiC*/Borosilicate#	C**/Borosilicate#
E_f	200 GPa	400 GPa	380 GPa
E_m	85 GPa	63 GPa	63 GPa
ν_f	0.3	0.3	0.3
ν_m	0.3	0.3	0.3
α_f	$3x10^{-6}/^oC$	$2.6x10^{-6}/^oC$	$0.1x10^{-6}/^oC$
α_m	$4x10^{-6}/^oC$	$3.2x10^{-6}/^oC$	$3.2x10^{-6}/^oC$
R	8 μm	70 μm	4 μm
K_m	2 MPa$\sqrt{m}$	0.75 MPa$\sqrt{m}$	0.75 MPa$\sqrt{m}$
γ_m	23.5 J/m^2	4.46 J/m^2	4.46 J/m^2
G_m	47 J/m^2	8.92 J/m^2	8.92 J/m^2
V_f	0.5	0.17	0.4 and 0.45
ΔT	-1200 ^oC	-500 ^oC	-500 ^oC
τ	2 MPa	10 MPa	10-25 MPa

+ Nicalon @ Data from Ref [2] * SCS-6 AVCO

#Corning-7740 ** Hercules Type HMU

TABLE 2 EXPERIMENTAL AND PREDICTED MCIS

Specimens	Experiment	ACK Model	Flaw-Inter. Model@
SiC/LAS	370±10 MPa	265 MPa (τ=2 MPa)	633 MPa (b/d=0)#
50 v%			377 MPa (b/d=1)#
SiC/Borosilicate	65±5 MPa	71.5 MPa (τ=10)	150 MPa (a=20μm)*
17 v%			61 MPa (a=120μm)*
C/Borosilicate	330±20 MPa	490 MPa (τ=10)	344 MPa (b/d=0)#
40 v%		665 MPa (τ=25)	337 MPa (b/d=0.1)#
C/Borosilicate	360±2 MPa	584 MPa (τ=10)	436 MPa (b/d=0)#
45 v%		792 MPa (τ=25)	376 MPa (b/d=0.1)#

@ Model provides estimated upper and lower bounds.

Size of matrix flaw is taken as that corresponds to maximum energy release rate in the range of $0 < a < t$.

* Size of interface flaws has no effect; size range of matrix flaw is based on tests of bulk borosilicate specimens.

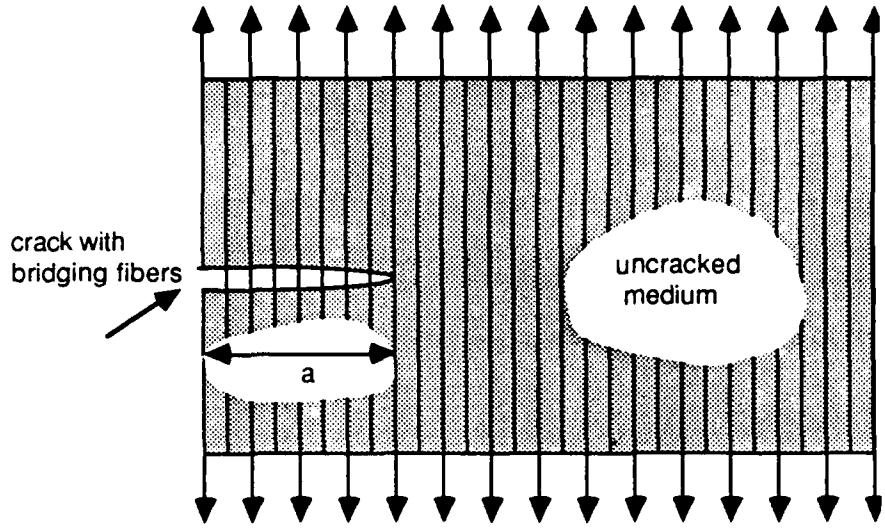

Fig. 1 Schematic representation of the fiber-bridged (ACK) model.

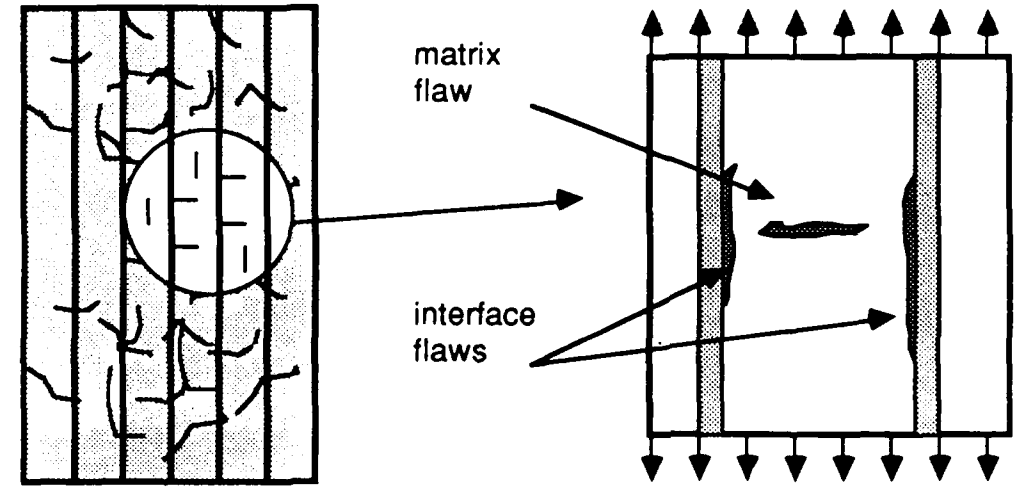

unidirectional composite
with manufacturing flaws

idealized local flaws and
interaction configuration

Fig. 2 Schematic representation of the flaw-interaction model

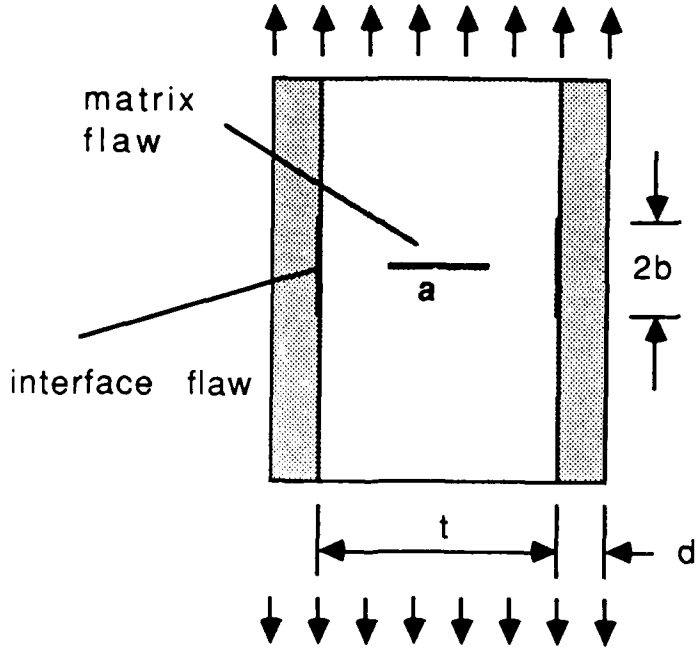

Fig. 3 A unit-cell of the flaw-interaction model

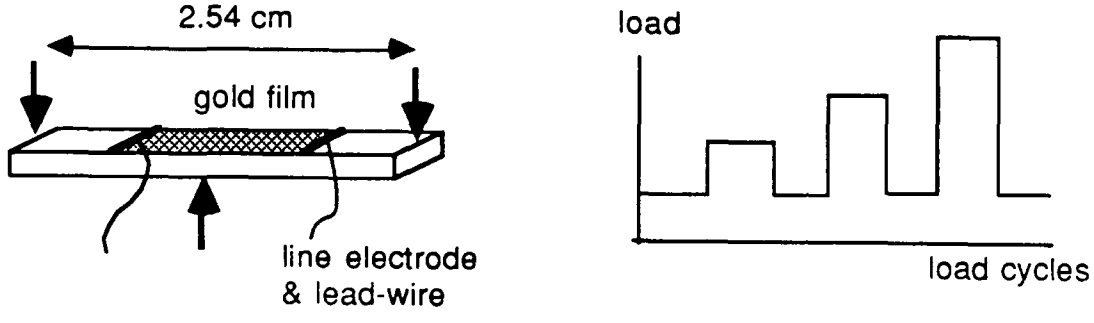

Fig. 4 Test specimen, gold-film, line electrodes and applied loading relationships, left; Applied step-loading cycles, right.

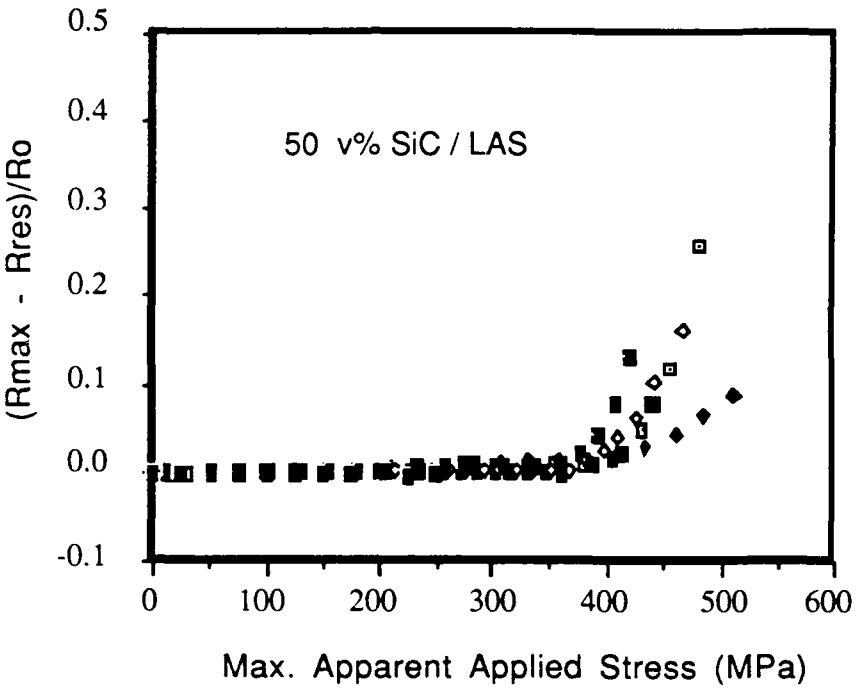

Fig. 5 Measured resistance change vs. the applied composite stress.
For SiC/LAS specimens with 50 v% Nicalon fibers.

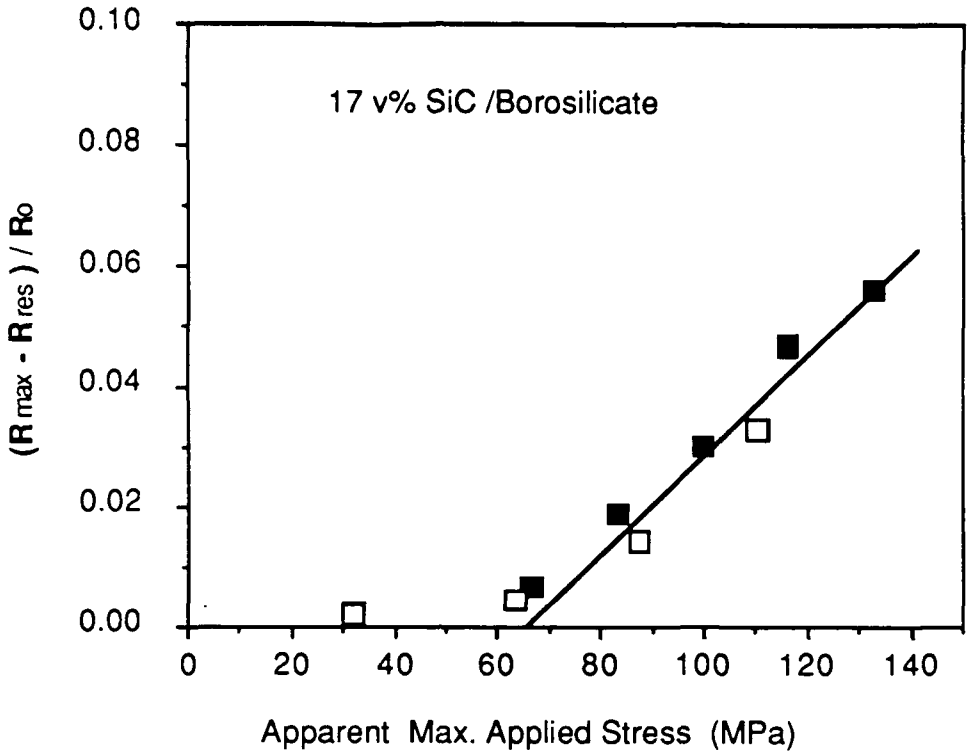

Fig. 6 Measured resistance change vs. the applied composite stress.
For SiC/Borosilicate specimens with 17 v% AVCO fibers.

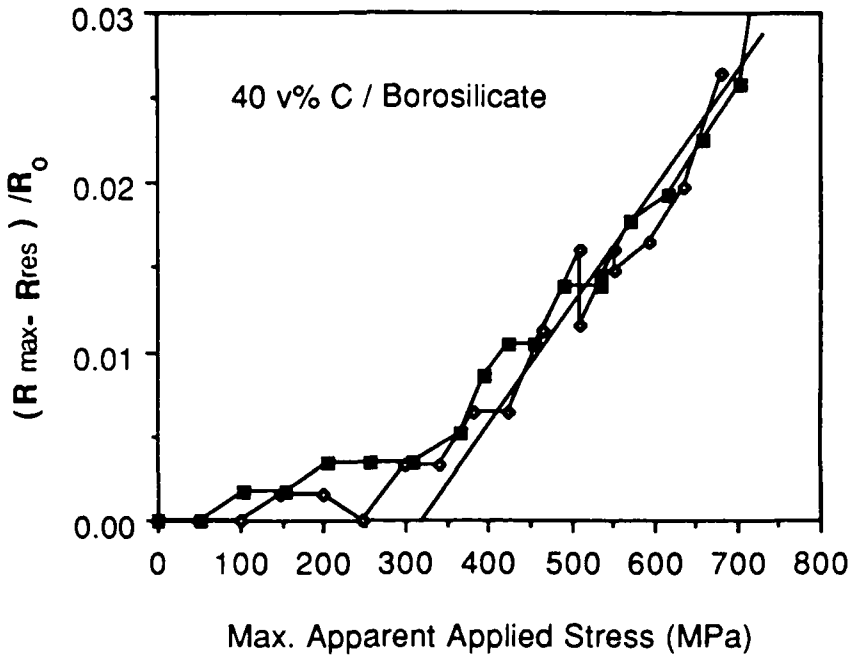

Fig. 7 Measured resistance change vs. the applied composite stress. For C/Borosilicate specimens with 40 v% Carbon fibers.

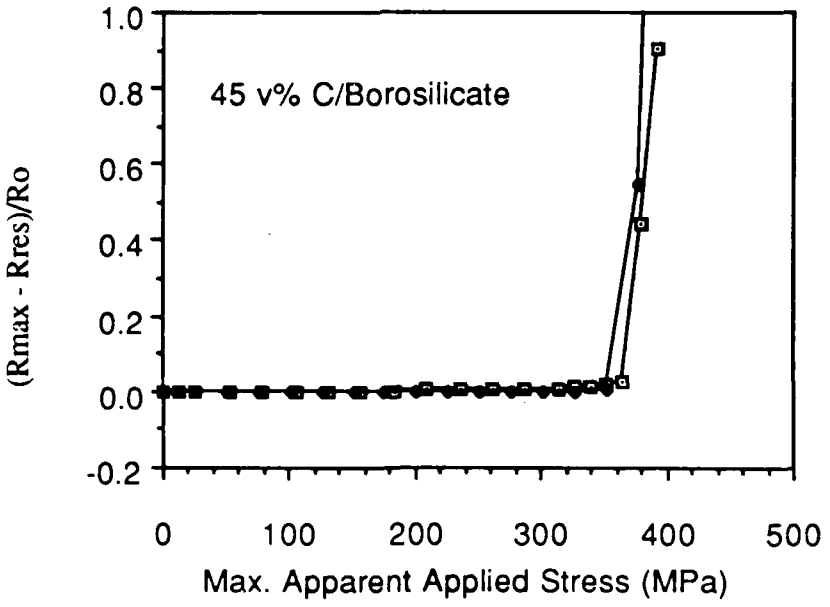

Fig. 8 Measured resistance change vs. the applied composite stress. For C/Borosilicatespecimens with 45 v% Carbon fibers.

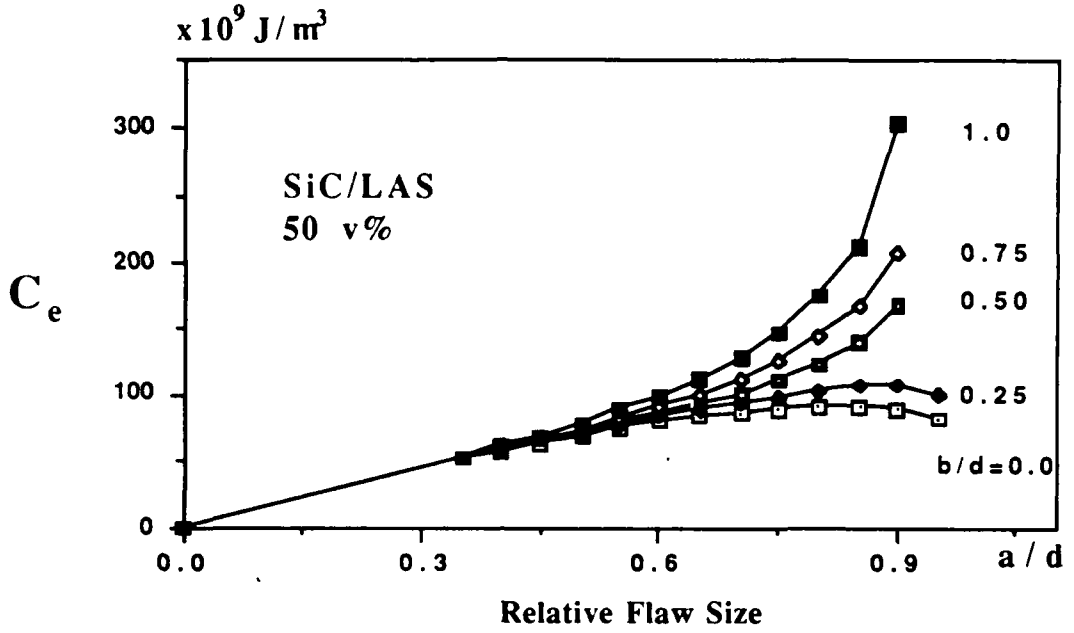

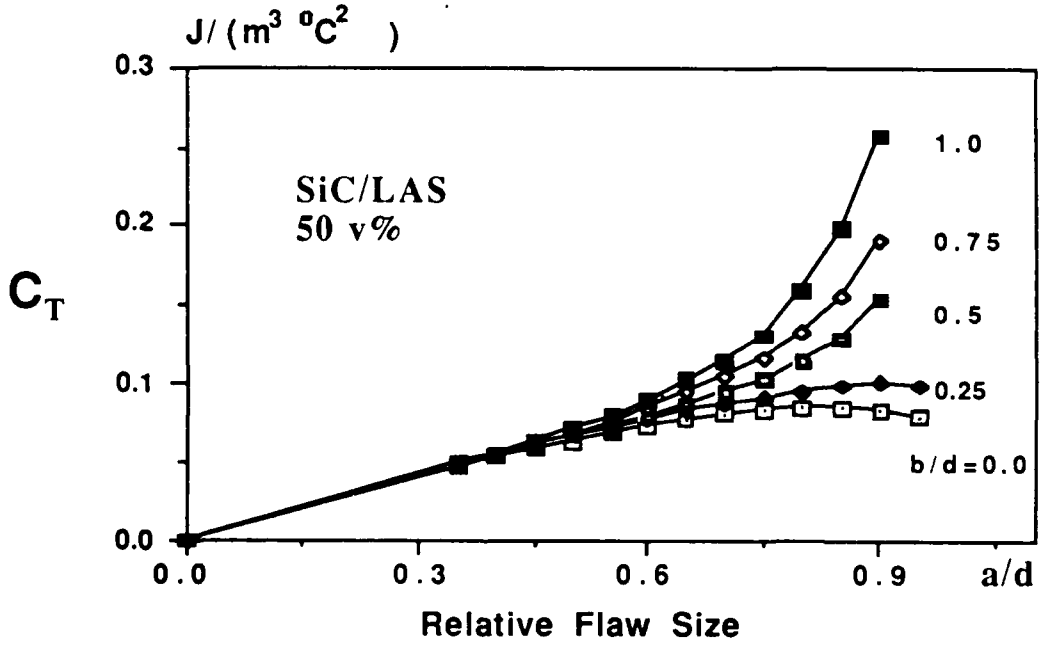

Fig. 9 Strain Energy Release Rate Coefficients for the SiC/LAS system (a) above: coefficient C_e and (b) below: coefficient C_T.

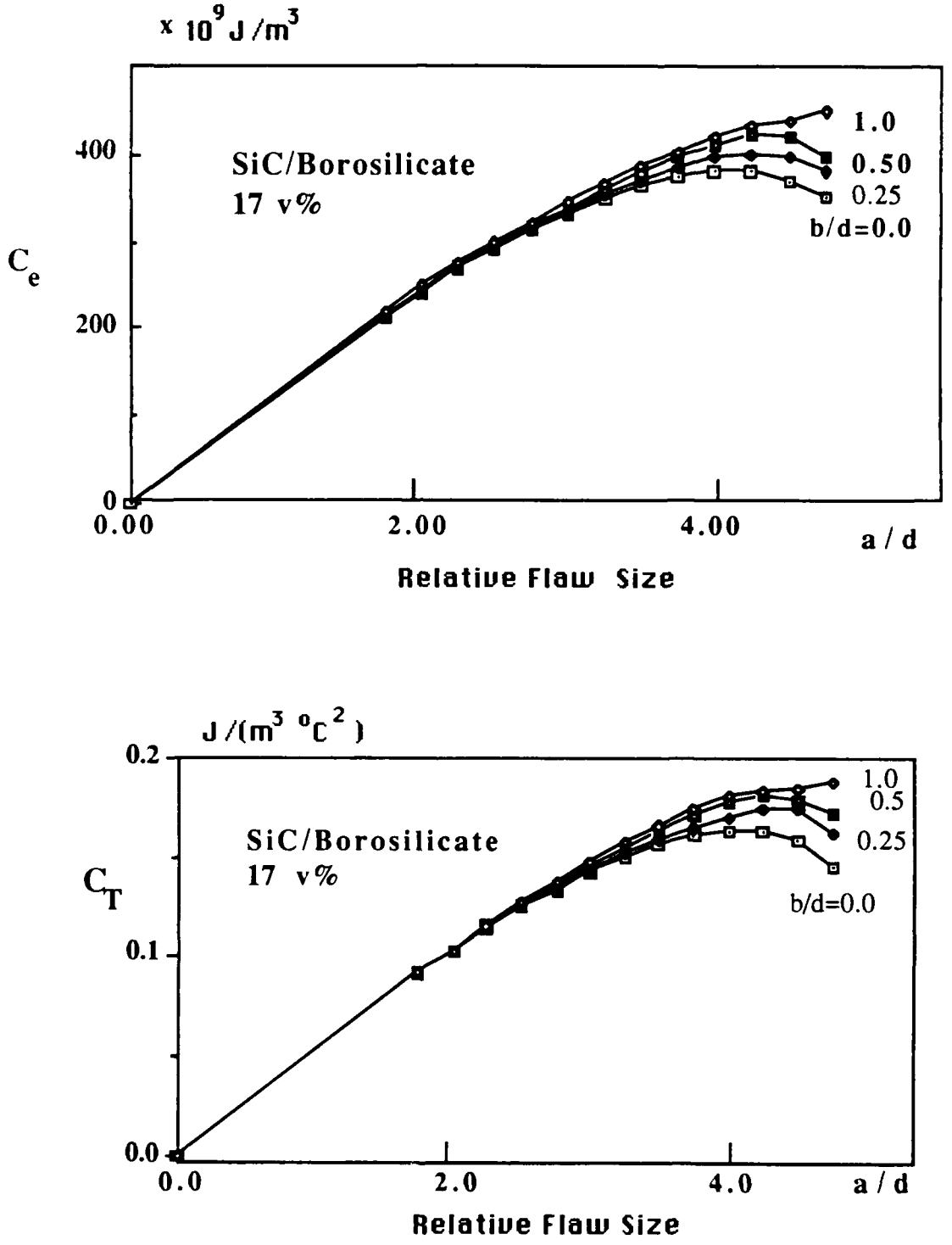

Fig. 10. Strain Energy Release Rate Coefficients for the SiC/Borosilicate system. (a) above: coefficient C_e and (b) below: coefficient C_T.

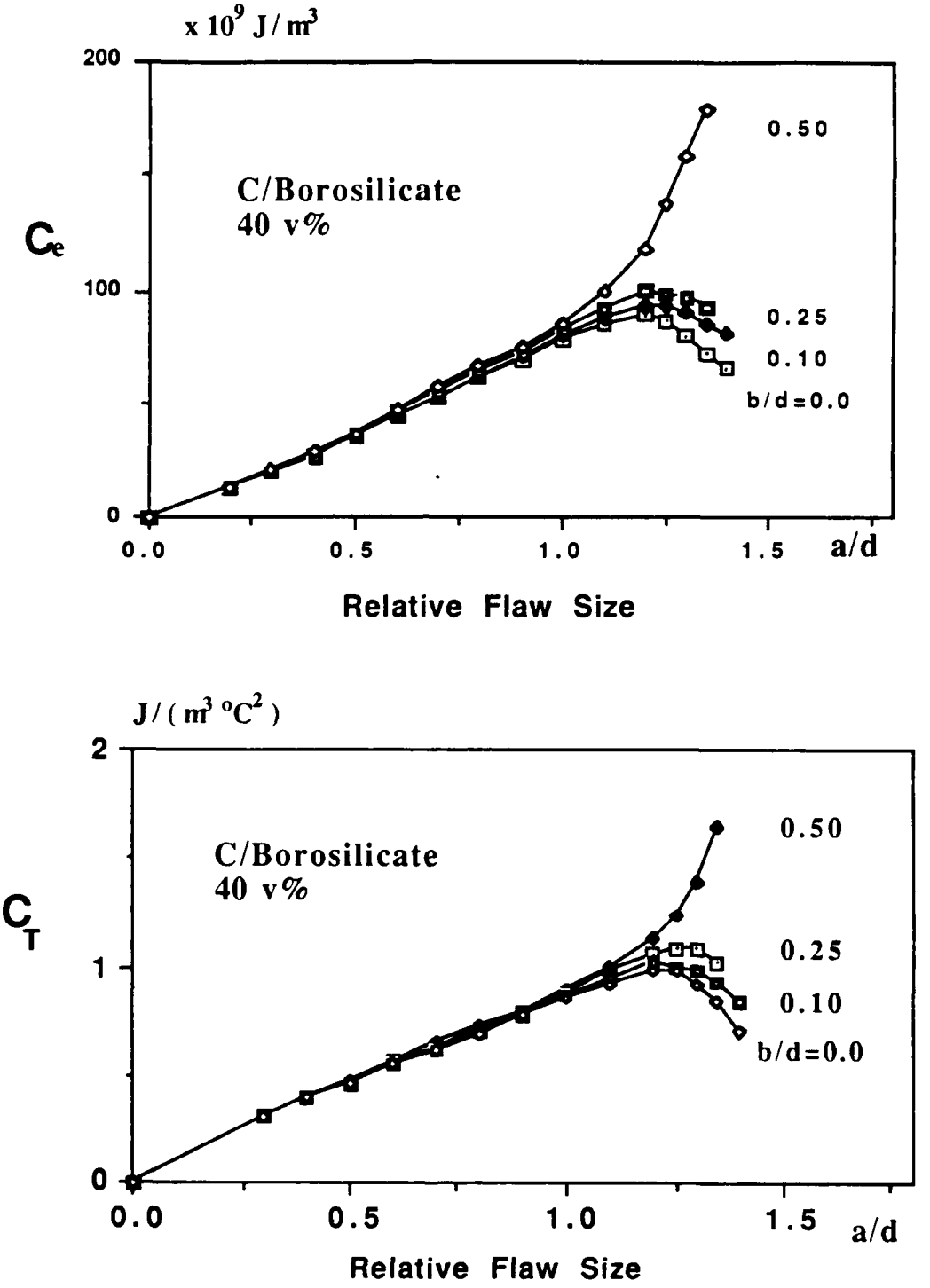

Fig. 11 Strain Energy Release Rate Coefficient for the C/Borosilicate system with 40 v%. (a) above: coefficient C_e and (b) below: coefficient C_T.

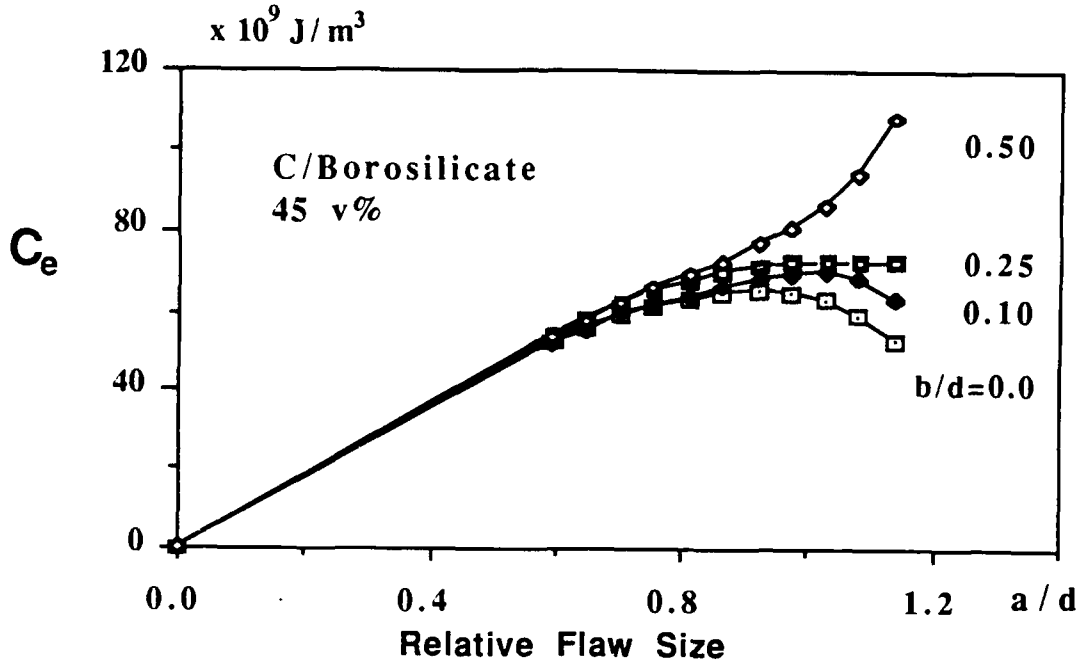

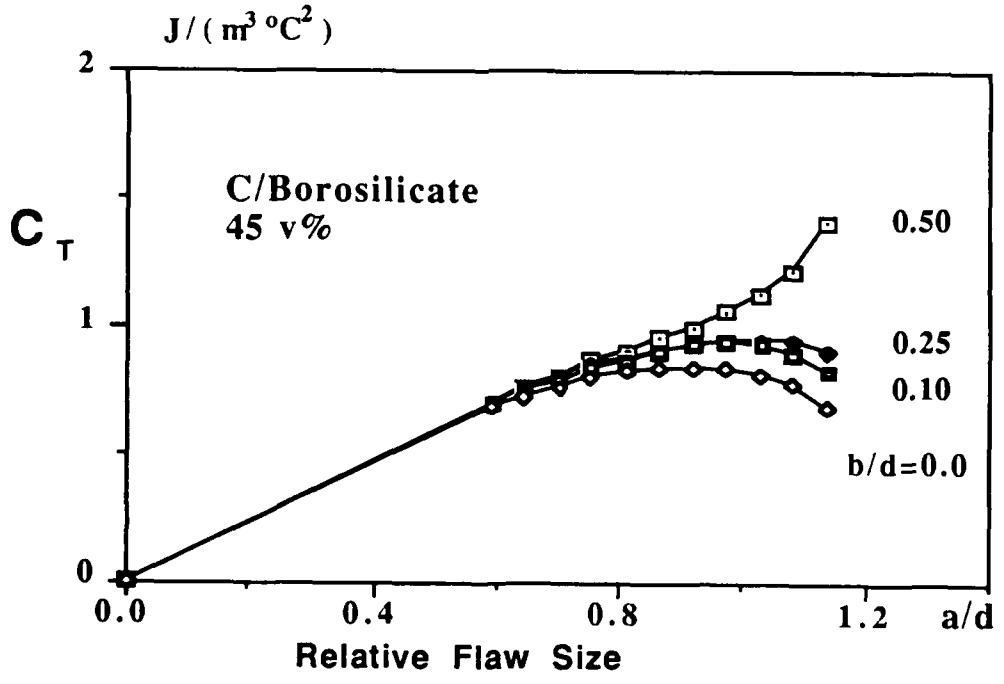

Fig. 12 Strain Energy Release Rate Coefficient for the C/Borosilicate system with 45 v%. (a) above: coefficient C_e and (b) below: coefficient C_T.